ML-TDR-64-34

ULTRASONIC METHODS IN THE STUDY OF DEFORMATION IN SINGLE CRYSTALS

Technical Documentary Report No. ML-TDR-64-34

March 1964

Air Force Materials Laboratory
Research and Technology Division
Air Force Systems Command
Wright-Patterson Air Force Base, Ohio

Project No. 7360, Task No. 736002

(Prepared under Contract No AF33(657)-8324 by the
Metals Research Laboratory, Brown University, Providence, R. I.
Bruce Chick, Akira Hikata, George Anderson
Charles Elbaum and Rohn Truell, authors)

FOREWORD

This report was prepared by the Metals Research Laboratory, Division of Applied Mathematics, Brown University, Providence, Rhode Island under USAF Contract No. AF33(657)-8324. This contract was initiated under Project No. 7360, "The Chemistry and Physics of Materials", Task No. 736002, "Nondestructive Methods". The work was administered under the direction of the AF Materials Laboratory, Research and Technology Division, with Mr. W. L. Shelton acting as the project engineer.

This report covers work conducted from January 1, 1963 to December 31, 1963, and is a continuation of work done under Contract No. AF33(616)-6945.

We are indebted to Mr. Richard Rowand for direct assistance and for encouragement in connection with this work.

ABSTRACT

The purpose of this investigation is that of understanding the physical changes which occur in aluminum and in certain ionic crystals during and after deformation. The investigation involves the study of imperfection behavior generally, and specifically the interaction of point defects with moving and vibrating dislocations, as well as the contribution of dislocations to the anharmonic characteristics of solids.

In the past year a hitherto unreported contribution of dislocations to the anharmonic behavior of solids was found. This effect was explained in terms of dislocation loop characteristics, in the presence of an external static stress combined with an ultrasonic stress. Experiments on this effect were carried out as a function of static stress, dislocation loop length, crystallographic orientation, plastic deformation and ultrasonic stress amplitude. The results of these experiments are consistent with the proposed theory.

Experiments were carried out on the relation between changes of electrical conductivity and ultrasonic attenuation in alkali halides. The effects of plastic deformation and of temperature on this relation were studied. A different time dependence at a given temperature was found for the conductivity change and for the attenuation change following plastic deformation. This difference is interpreted in terms of dependence of conductivity changes on the consideration of point defects in the lattice and on the dependence of the attenuation change on the number of point defects reacting with dislocations.

Preliminary experiments were conducted on the temperature dependence of the magnitude and sign of the surface charge developed in alkali halides. The difference of potential between two surfaces of a specimen, maintained at different temperatures, was measured as a function of the temperature difference and of the average temperature. The results were studied in terms of charge distribution associated with thermal and chemical diffusion currents.

Experiments were carried out on the recovery of ultrasonic attenuation following plastic deformation and as a function of plastic strain. The recovery theory which predicts a dependence of attenuation on the 2/3 power of time was extended to include the case of overdamped dislocation vibrations. A mechanism for attenuation recovery which takes into account point defect migration to the dislocations, followed by the escape of these defects to sinks along the dislocations was considered in some detail.

An Automatic Recording Time Measurement Unit (ARTMU) has been developed as an aid in obtaining rapidly changing velocity data during dynamic experiments. The unit has a time resolution of 1 part in 2×10^5 and is useable at any ultrasonic frequency where two or more high stability echoes are available from the particular sample under investigation.

This technical documentary report has been reviewed and is approved.

W. J. TRAPP
Chief, Strength and Dynamics Branch
Metals and Ceramics Division
Air Force Materials Laboratory

TABLE OF CONTENTS

LIST OF ILLUSTRATIONS

I. The Effect of Dislocations on Finite Amplitude Ultrasonic Waves in Aluminum

Introduction

This section is concerned with the contribution of dislocations to the anharmonic properties of solids. These properties manifest themselves through the generation of higher harmonics of a wave propagating in the medium.

When a sinusoidal ultrasonic wave of a given frequency and of sufficient amplitude is introduced into a non-linear or anharmonic solid, the fundamental wave will distort as it propagates, so that the second and higher harmonics of the fundamental frequency will be generated. Measurements of the amplitude of these harmonics provide information on the coefficients of the second and higher order terms of the stress-strain relation (1) for a non-linear solid. In the general case, the complete tensor form of the stress-strain relation is used and the corresponding equations of motion must be solved in three dimensions. For the purpose of the present study, however, it is sufficient to consider the simpler one dimensional case of a plane compressional wave propagating in the x direction. Furthermore, it will be assumed that the non-linear stress-strain relation can be represented by the first three terms of a power series, i.e.

$$\sigma = A\varepsilon + \frac{B}{2}\varepsilon^2 + \frac{C}{3}\varepsilon^3 \qquad (1)$$

where σ is the stress, ε is the strain and A, B, C are the elastic constants of second, third and fourth order respectively.

When a compressional wave $u = A_{10} \sin \omega t$ is introduced into a non-linear solid whose stress-strain relation can be described by equation (1), the equation of motion for the wave is

$$\rho \frac{\partial^2 u}{\partial t^2} = A \frac{\partial^2 u}{\partial x^2} + B \frac{\partial u}{\partial x} \cdot \frac{\partial^2 u}{\partial x^2} + C \left(\frac{\partial u}{\partial x}\right)^2 \frac{\partial^2 u}{\partial x^2} \qquad (2)$$

which is obtained by substituting $\frac{\partial \sigma}{\partial x}$ from equation (1) in the wave equation

$$\rho \frac{\partial^2 u}{\partial t^2} = \frac{\partial \sigma}{\partial x} \qquad (3)$$

---

(1) This relation is usually obtained from a Taylor series expansion of the strain energy function in terms of displacement gradients.

Manuscript released by the authors March , 1964 for publication as a ML Technical Documentary Report.

The non-linear differential equation (2) can be solved approximately by iteration. When two iterations are performed, the following result is obtained:

$$u(x,t) = A_{10} \sin(kx - \omega t) - \frac{1}{8}\cdot\frac{B}{A}\cdot(A_{10}k)^2 \cdot x \cdot \cos 2(kx - \omega t)$$

$$- \frac{1}{32} \cdot \frac{B^2}{A^2} \cdot (A_{10}\cdot k)^3 \cdot k \cdot x^2 \quad [\sin 3(kx - \omega t) + \sin (kx - \omega t)] \qquad (4)$$

$$+ \frac{1}{16} \cdot \frac{B^2}{A^2} \cdot (A_{10}k)^3 \cdot x \cdot \left[\frac{2}{3}\cos 3(kx - \omega t) + \cos (kx - \omega t)\right]$$

$$- \frac{1}{24} \cdot \frac{C}{A} (A_{10} \cdot k)^3 \cdot x \quad [\cos 3(kx - \omega t) + 3 \cos (kx - \omega t)] + \ldots\ldots$$

where k is the wave vector and x is the distance the wave has traveled. From this solution one obtains the expression for the amplitude of the second harmonic A_2 in the following form:

$$A_2 = \frac{1}{8} \cdot \frac{B}{A} (A_{10}\, k)^2 \cdot x \qquad (5)$$

The problem must now be further specialized by defining the different contributions to the strain ε of the solid subjected to an external stress. In most metals the non-linearity of the stress-strain relation (deviation from Hooke's law) may arise from two causes. One is the anharmonicity of the lattice and the other is the contribution of the non-linear part of the stress-strain relation for dislocation displacement. The lattice anharmonicity is a well known phenomenon which has been studied extensively through phonon-phonon interactions, thermal expansion and other physical properties. The non-linear part contributed by dislocation displacement has not been hitherto explored and constitutes the main object of the present study.

If in addition to the ultrasonic wave, the solid is subjected to a small uniaxial stress glide displacement of the dislocations will contribute to the overall strain. The dislocation displacements are expected to occur in metals, and to contribute to the non-linearity, for static stresses lower than those required to affect the lattice anharmonicity. This means that by investigating the higher order harmonics generated in a specimen, as a function of a bias stress, it should be possible to study the contribution of dislocations to the anharmonic behavior of solids. More specifically, it should also be possible to use this method in analyzing the early stages of deformation as well as the dislocation damping mechanism.

Non-Linear Effects Due to Dislocation Displacements

In order to derive a relation between applied stress and displacement of a dislocation, consider an edge dislocation lying in a slip plane of an isotropic crystal. When a longitudinal stress σ having a shear stress component $\tau = R\sigma$ in the slip plane, along the slip direction is applied to the crystal, the dislocation will be displaced (R is the resolving shear factor). If the stress is small enough and the dislocation is pinned at the points 2L cm apart (loop length 2L), then the dislocation line will bow out like a string and take the form of an arc of a circle of radius r. When the dislocation density is small so that the interaction between dislocations can be neglected, and the line tension T can be considered to be independent of the radius of curvature and be equal to $\mu b^2/2$, then

$$\tau = \frac{T}{rb} = \frac{\mu b}{2r} \qquad (6)$$

where μ is the shear modulus and b is Burgers vector (Fig. 1). The corresponding shear strain γ_d caused by the displacement of the dislocation is given by

$$\gamma_d = \frac{\lambda b}{2L} \cdot S \qquad (7)$$

where λ is the effective dislocation density and S is the area swept out by each dislocation loop which is given by

$$S = r^2\left(\theta - \tfrac{1}{2}\sin 2\theta\right) \qquad (8)$$

From equations (6), (7) and (8) one obtains the shear stress-shear strain relationship associated with dislocation displacement,

$$\gamma_d = \frac{2}{3}\frac{\lambda L^2}{\mu}\tau + \frac{4}{5}\frac{\lambda L^4}{\mu^3 b^2}\tau^3 \qquad (9)$$

where the first and third power of (L/r) in the series expansion of $\mathrm{Sin}^{-1}(\frac{L}{r})$ are retained (2). The lattice strain ε_ℓ of the crystal due to the uniaxial stress σ is given by

$$\sigma = E_1 \varepsilon_\ell - E_2 \varepsilon_\ell^2 \qquad (10)$$

(2) At this stage of analysis the stress range is considered within the region where r is larger than L. When r becomes equal to L, further increase of stress expands the dislocation loop spontaneously, and the loop length 2L for the particular dislocation becomes meaningless.

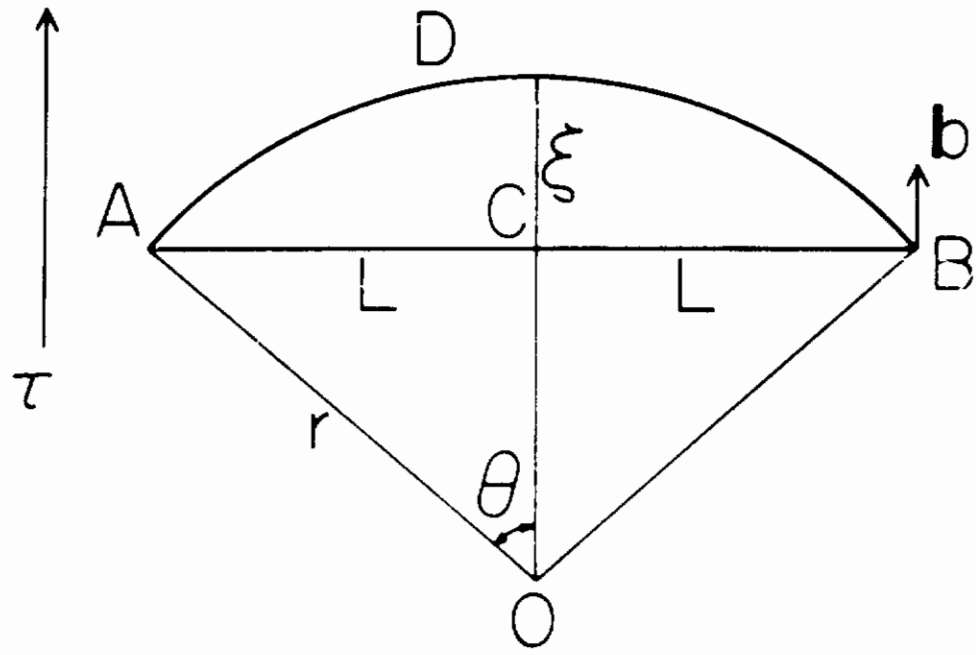

Figure 1. Bowed-out Dislocations ADB
τ: Shear Stress
r: Radius of Curvature
2L: Dislocation Loop Length
b: Burgers Vector

where E_1 and E_2 are the appropriate moduli of the second and third order respectively. Thus the total longitudinal strain ε becomes

$$\varepsilon = \varepsilon_\ell + R\,\gamma_d \tag{11}$$

From equation (9), (10) and (11) one obtains, after making some approximations, the longitudinal stress-longitudinal strain relation for the material

$$\varepsilon = \left(\frac{1}{E_1} + \frac{2}{3}\cdot\frac{\lambda L^2 R^2}{\mu}\right)\cdot\sigma + \frac{E_2}{E_1^3}\cdot\sigma^2 + \frac{4}{5}\cdot\frac{\lambda L^4 R^4}{\mu^3 b^2}\cdot\sigma^3 + \ldots\ldots \tag{12}$$

Amplitude of the Second Harmonic

When a small stress $\Delta\sigma$ is applied in addition to the stress σ, the dislocation will be displaced further causing additional strain $\Delta\varepsilon$. In such a case,

$$\Delta\sigma = \frac{\partial\sigma}{\partial\varepsilon}\cdot(\Delta\varepsilon) + \frac{1}{2}\cdot\frac{\partial^2\sigma}{\partial\varepsilon^2}\cdot(\Delta\varepsilon)^2 + \frac{1}{6}\cdot\frac{\partial^3\sigma}{\partial\varepsilon^3}\cdot(\Delta\varepsilon)^3 + \ldots\ldots \tag{13}$$

$$\simeq \frac{1}{\frac{1}{E_1} + \frac{2}{3}\cdot\frac{\lambda L^2 R^2}{\mu}}\cdot(\Delta\varepsilon) - \frac{\frac{E_2}{E_1^3} + \frac{12}{5}\cdot\frac{\lambda L^4 R^4}{\mu^3 b^2}\cdot\sigma}{\left(\frac{1}{E_1} + \frac{2}{3}\cdot\frac{\lambda L^2 R^2}{\mu}\right)^3}\cdot(\Delta\varepsilon)^2 + \ldots\ldots$$

which provides the stress strain relation for the small stress $\Delta\sigma$ under the influence of a biasing stress σ.

By comparing the above equation (13) with equation (1), one obtains the following relations between the coefficients

$$A = \frac{1}{\frac{1}{E_1} + \frac{2}{3}\cdot\frac{\lambda L^2 R^2}{\mu}}$$

$$B = - \frac{2\left(\frac{E_2}{E_1^3} + \frac{12}{5} \cdot \frac{\lambda L^4 R^4}{\mu^3 b^2} \cdot \sigma\right)}{\left(\frac{1}{E_1} + \frac{2}{3} \cdot \frac{\lambda L^2 R^2}{\mu}\right)^3}$$

Using the above quantities one obtains, from expression (5), the following expression for the amplitude of the second harmonic:

$$A_2 = \frac{1}{4} \cdot \frac{\frac{E_2}{E_1^3} + \frac{12}{5} \cdot \frac{\lambda L^4 R^4}{\mu^3 b^2} \cdot \sigma}{\left(\frac{1}{E_1} + \frac{2}{3} \frac{\lambda L^2 R^2}{\mu}\right)^2} \cdot (A_{10} \cdot k)^2 \cdot x \qquad (14)$$

The above analysis, however, does not take into account the fact that the induced fundamental wave as well as the higher harmonics generated by dislocations are attenuated as they propagate along the crystal. In order to take this effect into account, consider a small segment of the crystal of thickness dx, Figure 2. The amplitude $A_{10,x}$ of the fundamental wave at the distance x is

$$A_{10,x} = A_{10} \cdot e^{-\alpha_1 x}$$

where α_1 is the attenuation coefficient of the fundamental wave (nepers/cm). The amplitude of the second harmonic $A_{2,x}$ generated in this segment dx is given by

$$A_{2,x} = K \cdot (A_{10,x})^2 \cdot dx,$$

where K is a constant (the factors appearing in the expression (14) except A_{10} and x). The amplitude A_{2x} decreases while it propagates from x to ℓ (the other end of the specimen, where the receiving transducer is placed) because it also suffers an attenuation α_2(3). Therefore, at the receiving end of the specimen, the amplitude of the second harmonic becomes

$$[K \cdot (A_{10,x})^2 \cdot dx\ ] \cdot e^{-\alpha_2(\ell - x)}$$

---

(3) Since the generation of the higher harmonic depends on the amplitude of the fundamental wave, the attenuation coefficient itself should be a function of x. However, energy transferred to the higher harmonics is expected to be much smaller than the energy loss due to other sources such as dislocation damping (which is considered to be independent of the strain-amplitude considered here). Therefore, the attenuation coefficient is treated as a constant along the axis.

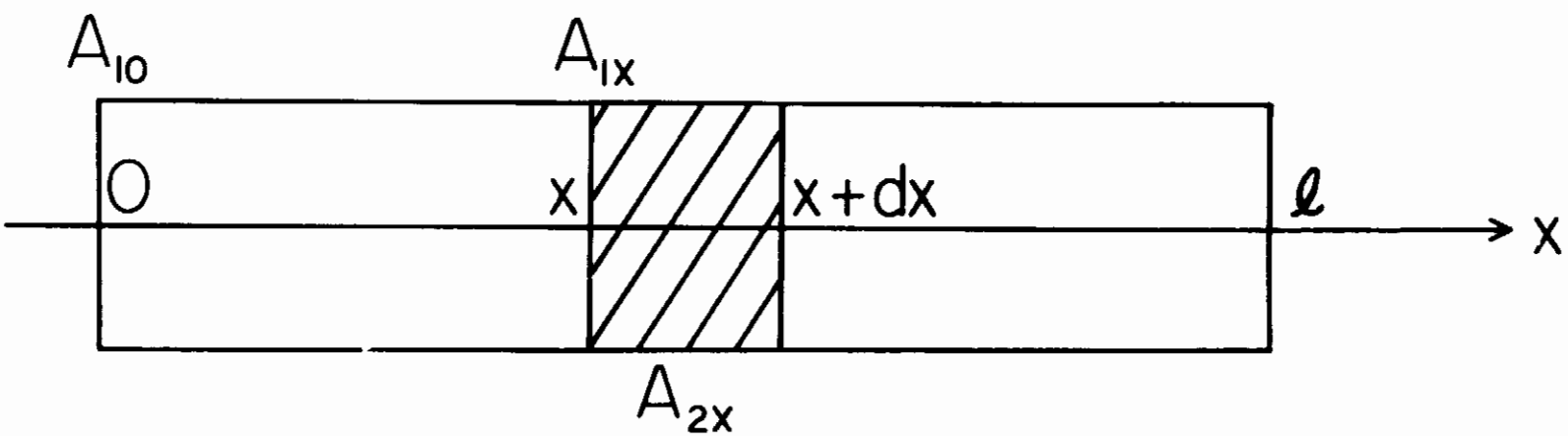

Figure 2. Generation of the Second Harmonic in the Small Segment dx of a Specimen
x is the Direction of Wave Propagation
ℓ is the length of the Specimen

Thus, the actual amplitude of the second harmonic A_2 becomes

$$A_2 = \int_0^{\ell} [K \cdot (A_{10,x})^2 \cdot dx] \cdot e^{-\alpha_2(\ell - x)}$$

$$= K \cdot (A_{10})^2 \cdot \frac{e^{-2\alpha_1 \ell} - e^{-\alpha_2 \ell}}{\alpha_2 - 2\alpha_1} \qquad (15)$$

When α_1 and α_2 are small, equation (15) reduces to equation (14).

Several features are apparent in these expressions, some of which are discussed in the following.

When the term $2/3 \cdot (\lambda L^2 R^2 / \mu)$ in equation (14) can be neglected compared with the term $1/E_1$ (which is true in most cases), the expression for the amplitude of the second harmonic is further simplified,

$$A_2 = \frac{1}{4} \cdot \left[\frac{E_2}{E_1} + \frac{12}{5} \cdot \frac{E_1^2 \lambda L^4 R^4}{\mu^3 b^2} \cdot \sigma\right] \cdot (A_{10} \cdot k)^2 \cdot \frac{e^{-2\alpha_1 \ell} - e^{-\alpha_2 \ell}}{\alpha_2 - 2\alpha_1} \qquad (16)$$

In equation (16), the amplitude of the second harmonic due to the lattice anharmonicity is represented by the term E_2/E_1, and that due to dislocation displacement is represented by the term

$$\frac{12}{5} \cdot \frac{E_1^2 \lambda L^4 R^4}{\mu^3 b^2} \cdot \sigma$$

The latter increases linearly with the applied static (biasing) stress σ and dislocation density λ, and the fourth power of the loop length L. For reasonable numerical values of these quantities such as $\lambda = 10^6$ cm/cm^3, $L = 2 \times 10^{-4}$ cm, $\mu = 3 \times 10^{11}$ dynes/cm^2, $b = 3 \times 10^{-8}$ cm, $A_{10} = 5 \times 10^{-9}$ cm, $x = 10$ cm and $k = 1.2 \times 10^2$ cm^{-1} (for 10 mc/sec. wave), the value of A_2 is

$$A_2 = (1 + 1.2 \times 10^{-6} \cdot \sigma) \times 10^{-12} \text{ cm}$$

This indicates that the dislocation term reaches the same order of magnitude as the lattice term at a biasing stress of about 10^6 dynes/cm^2, and is about three orders of magnitude smaller than the amplitude of the fundamental wave. Both terms increase with the square of the amplitude A_{10}. The amplitude A_2, equ. (15) has a maximum at the distance $(x_2)_{max}$ (from the driving transducer) determined by the following relation

$$(x_2)_{max} = \frac{\ell \, n \frac{2\alpha_1}{\alpha_2}}{2\alpha_1 - \alpha_2} \qquad (17)$$

This means that when the specimen length is properly chosen according to the attenuation values of the material, a maximum in amplitude should be observed in the echo train obtained by the pulse echo method.

It is also clear that the amplitude of the second harmonic increases with the second power of the fundamental frequency ω, ($k = \omega/V$, where V is the velocity of the wave), provided that the attenuation α_1 and α_2 remain unchanged. In practise, however, the attenuation also increases with frequency and there should be an optimum frequency in which the energy transfer from the fundamental to the second harmonic is largest for the given material and the size of the specimen.

Experimental Procedures and Results

Stress Dependence

In order to investigate the concept outlined above, the following experiment was performed. On one end of the specimen (aluminum single crystal, 99.99 + % pure, 0.95 cm x 0.95 cm and 12.7 cm long, axis of the rod coincided with <100> crystallographic direction) a 10 Mc/sec quartz transducer was mounted as a transmitter and receiver of a 10 Mc/sec fundamental pulsed wave (4), and on the other end a 20 Mc/sec transducer was bonded as a receiver for the second harmonic (20 Mc/sec) generated in the specimen. The 10 Mc/sec and the 20 Mc/sec signals were received, amplified and displayed by two independent electronic setups. In the absence of a uniaxial external stress, a 20 Mc/sec wave of small amplitude was generated when the fundamental was sufficiently large. These results were quite similar to the measurements reported by Breazeale and Thompson (5). Then the specimen was subjected to a tensile stress by hanging weights from the lower end of the specimen, and the attenuation change of the 10 Mc/sec fundamental wave at one end and the amplitude change of the first echo of the 20 Mc/sec wave received at the other end were measured as a function of the tensile stress. The results are shown in Figure 3. As the stress increases the attenuation of the 10 Mc/sec wave increases slightly while the amplitude of the first echo of the second harmonic increases quite rapidly in the beginning and then goes throug a maximum.

It should be pointed out that the tensile stresses on the specimen (as indicated in Figure 3) correspond to shear stress on the slip planes ranging from about 1 g/mm^2 to about 5 g/mm^2. These stresses constitute a small fraction of the macroscopic yield stress.

The generation of a second harmonic in the crystal indicates clearly that a non-linear mechanism operates in the solid. Of the two possibilities indicated earlier, namely lattice anharmonicity and dislocation displacements, the second appears to be predominant in the present case, for the following reasons. The static strain, corresponding to the external stress, is of the order of 10^{-6} to 10^{-5} (in the absence of dislocation displacements). For this strain an appreciable change in the value of the higher order coefficients (6) in the stress-strain relation of the lattice is not expected to occur and, therefore, there should be no appreciable increase of the amplitude of the second harmonic with applied stress. The observed increase (see Figure 3) can, however, be explained in terms of dislocation displacements, when the

(4) The pulse echo method was used in these experiments.
(5) M. A. Breazeale and D. O. Thompson; Applied Physics Letters, 3, 77 (1963)
(6) The coefficients of the square and higher order terms in strain, i.e. the anharmonic terms.

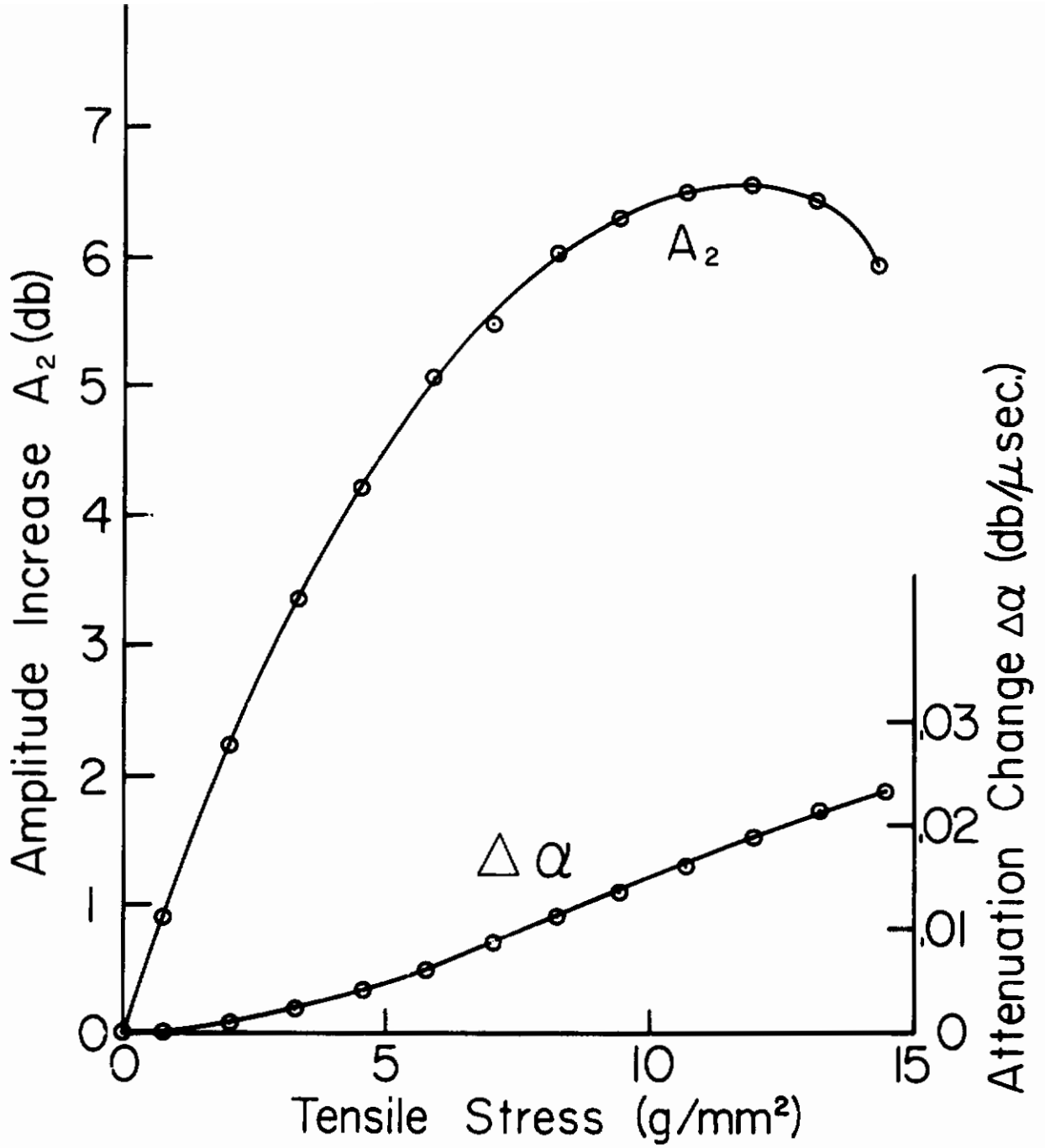

Figure 3. Effect of Bias Stress on the Amplitude of the Second Harmonic A_2 and the Attenuation of the Fundamental Wave $\Delta\alpha_1$ Aluminum Single Crystal, <100> Orientation.

stress-strain relation for dislocation strain is non-linear as shown in the preceding paragraphs. The qualitative physical model can be described as follows: When a tensile stress is applied to the specimen, the dislocations become curved. The additional oscillatory displacements of the dislocations from the curved configuration caused by the ultrasonic wave, involve a non-symmetric and non-linear stress-strain relation. Even power terms of strain in this relation will, therefore appear as a consequence of the asymmetry, i.e. the displacements of dislocations from the new equilibrium position are not the same for equal positive and negative values of stress.

The occurrence of the maximum in the amplitude A_2 as a function of applied stress σ may be explained qualitatively as follows. When the bias stresses are small, the dislocation loops (between pinning points) simply bow-out, giving a linear increase of the second harmonic amplitude with increasing bias stress. The increase of attenuation due to the increase of loop length from a straight line to a bowed-out configuration is expected to be insignificant. Under these conditions, that is, as long as there is no appreciable change in the attenuation, the amplitude changes of the second harmonic is determined by the bias stress (the term in α_1 and α_2, equation (16), remains essentially constant). As the bias stress increases, however, dislocations tend to break away from weak pinning points, which result in an appreciable increase in loop length. As can be seen from equation (16), an increase of loop length L produces two competing effects on the amplitude of the second harmonic; an increasing effect through the term

$$\frac{12}{5} \cdot \frac{E_1^2 \lambda L^4 R^4 \cdot \sigma}{u^3 b^2}$$

and a decreasing effect through the attenuation term

$$\frac{e^{-2\alpha_1 \ell} - e^{-\alpha_2 \ell}}{\alpha_2 - 2\alpha_1} .$$

where the attenuation coefficients α_1 and α_2 are also expected to be proportional to the fourth power of the loop length (7). Since the latter term is in exponential form, it will eventually become the determining factor. Thus the amplitude of the second harmonic starts decreasing as the bias stress becomes large enough to cause unpinning which results in a maximum in the $A_2 - \sigma$ relation.

Check of the Dependence on Dislocation Loop Length

In order to verify further the idea that dislocations are responsible for the generation of the second harmonic, experiments using polycrystalline specimen of a 2S alloy was conducted. To eliminate the geometrical factor, the specimen was made in the same shape and size as the single crystal specimen tested before (0.95 cm x 0.95 cm cross section and 12.7 cm long). When 10 Mc/sec compressional waves were introduced into the specimens, an appreciable amount of the second harmonic was observed, before applying any static stress. Then the specimens were subjected to tensile stresses up to 160 g/mm^2. The results are shown in Figure 4. No change of the second harmonic as a function of applied static stress, over a range from zero to 160 g/mm^2 is found in this case. Since the dislocation loop length in 2S aluminum is

(7) A. Granato and K. Lucke, Journal of Applied Physics 27, 583, 789 (1956)

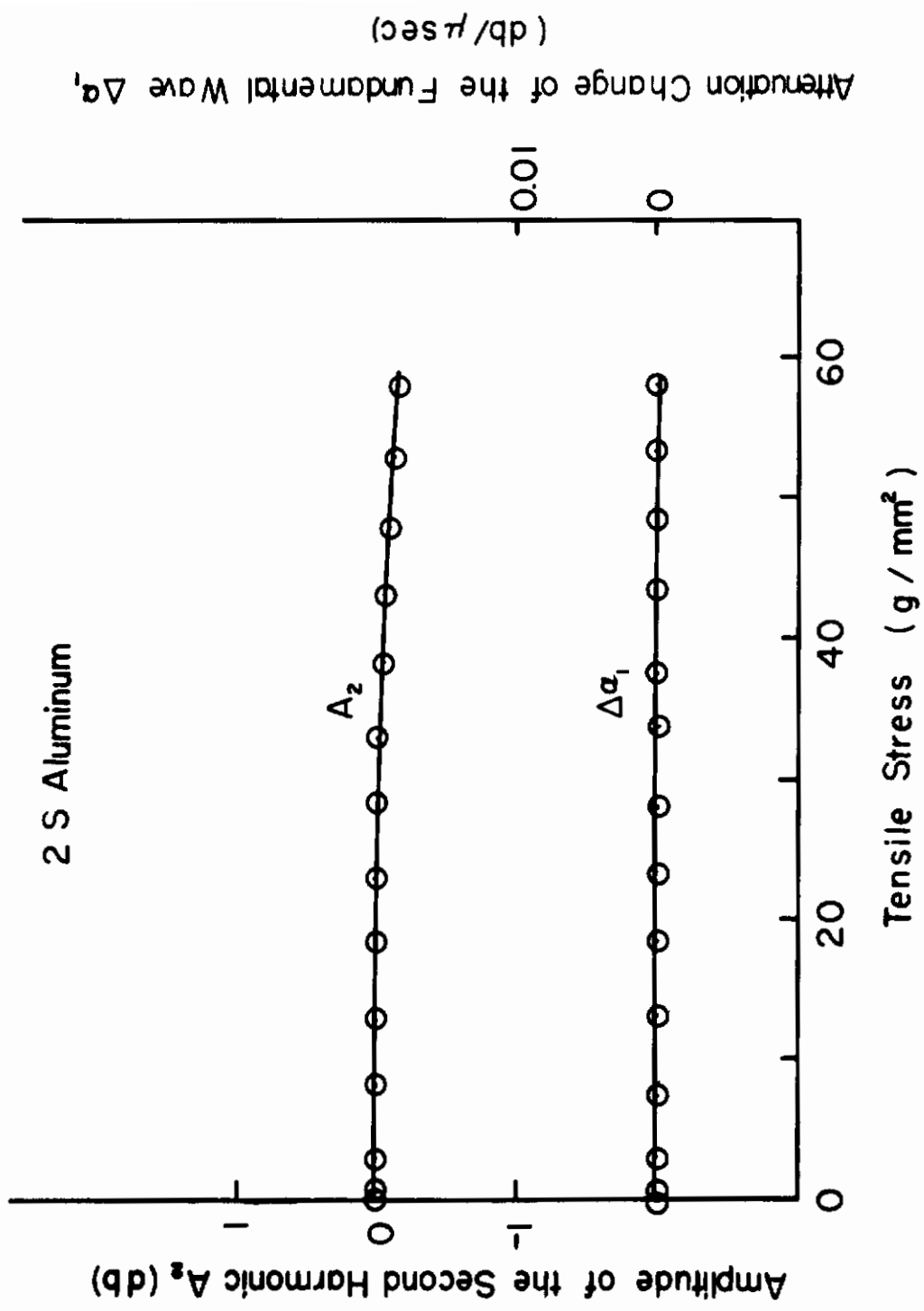

Figure 4. Effect of Bias Stress on the Amplitude of the Second Harmonic and the Attenuation of the Fundamental Wave. 2S Aluminum.

expected to be much shorter than that in the single crystal of high purity aluminum, the dislocation contribution to the generation of the second harmonic in this material is also expected to be small and not very sensitive to the applied stress. The above experiment, therefore, constitutes direct proof that the stress dependent part of the second harmonic observed in high purity single crystals is due to dislocation motion .

Check for Second Power Law

According to equation (16) the amplitude of the second harmonic is expected to be proportional to the square of the amplitude of the fundamental wave, as long as the attenuation change due to the generation of the higher harmonics can be considered to be negligible. This is demonstrated in Figure 5, 6, 7, 8 and 9 for the specimens of <100>, <110>, <111> crystallographic orientations, 2S aluminum and 11S aluminum respectively, where the amplitude of the second harmonic is plotted as a function of the square of the amplitude of the fundamental wave in db (logarithmic) scale. The results (straight line of slope one) confirm the second power relation between the amplitude of the second harmonic and the fundamental wave.

Effect of Plastic Deformation

In order to check the effect of the dislocation density, a comparison was made between fully annealed specimens and specimens slightly deformed (plastically) in tension in terms of the stress sensitivity of the amplitude of the second harmonic. The results together with the corresponding attenuation change are shown in Figure 10, 11 and Figure 12 for <100>, <111> and <110> orientation respectively for tensile stress, and Figure 13 for <100> orientation for compressional stress. It is clear that the plastic deformation definitely increased the amount of the amplitude change of the second harmonic. It is interesting to note that the amplitude change of the deformed specimen shows a maximum for the compressional stress (Figure 13) while, for the tensile stress, the amplitude change goes through a minimum (Figure 10, 11, 12). This observation can be explained by taking into account the fact that the dislocations in the deformed specimen are no longer straight lines, in the absence of an external stress, but are bowed out (due to the internal residual stress) in the direction of the external compressional stress. Therefore, when an external tensile stress is applied, the bowed out dislocations tend to become straight first, and then bow out again in the direction of the tensile stress. Since the amplitude of the second harmonic due to dislocations is expected to be zero when the dislocations are straight (equation 16), the amplitude of the second harmonic is also expected to go through a minimum as the tensile stress is increased. On the other hand, when an external compressional stress is applied, the dislocations will bow out further without going through the configuration of the straight line. Therefore, the amplitude of the second harmonic should start increasing as the compressional stress increases. There should be a maximum, however, because of the effect discussed in the paragraph "Effect of Static Stress". The amplitude change for the tensile stress goes through a maximum when further tensile stress is applied (Figure 14), again for the reason discussed in the paragraph "Effect of Static Stress".

Amplitude Dependent Attenuation

The effect of plastic deformation on the generation of higher harmonics is also clearly shown in the following experiments. Since more energy of the fundamental wave will be transferred to the higher harmonics as the amplitude of the fundamental wave increases, the attenuation of the fundamental wave is expected to increase accordingly. In order to investigate this effect, the attenuation of the fundamental is

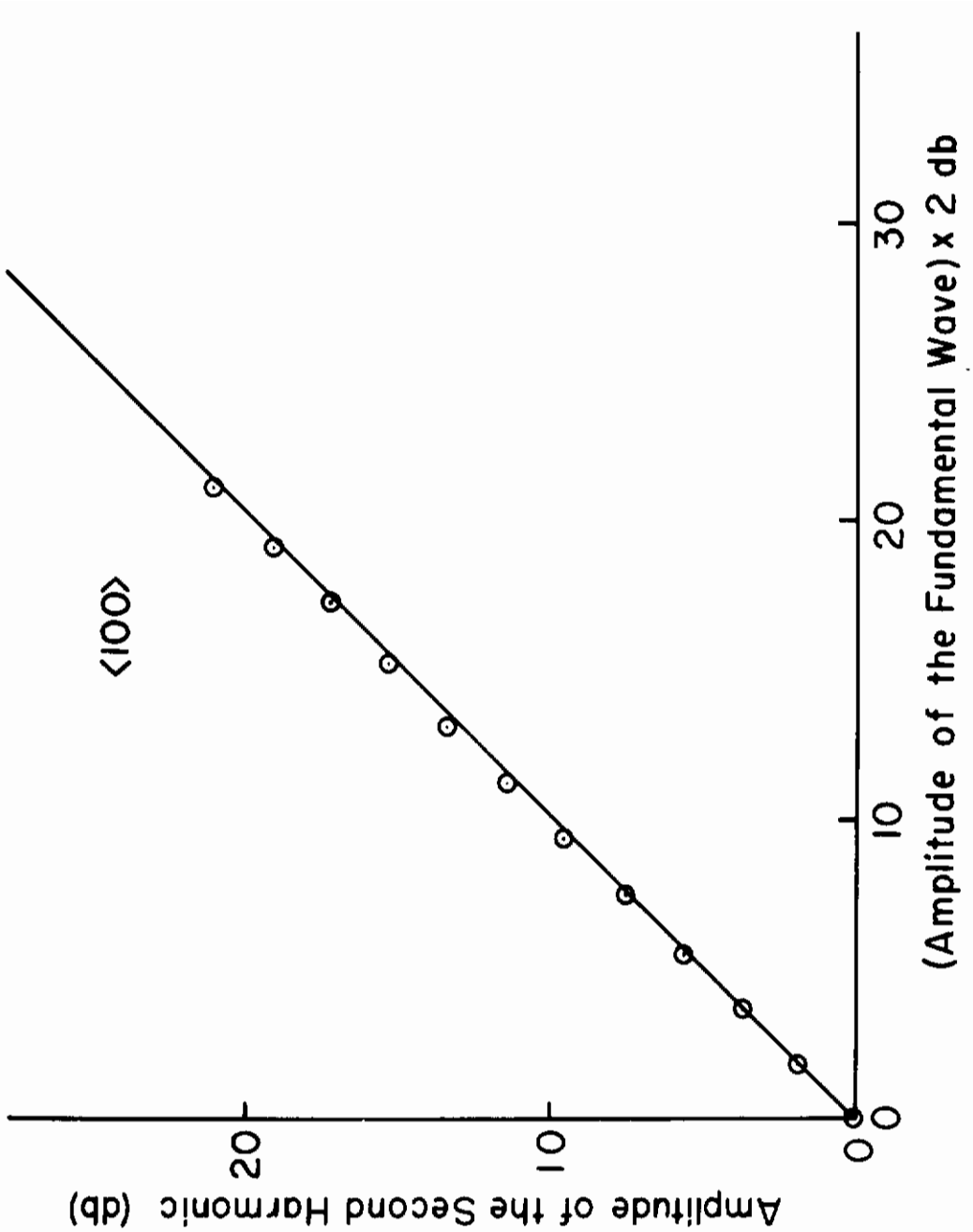

Figure 5. Amplitude of the Second Harmonic as a Function of the Amplitude of the Fundamental Wave. Aluminum Single Crystal, <100> Orientation.

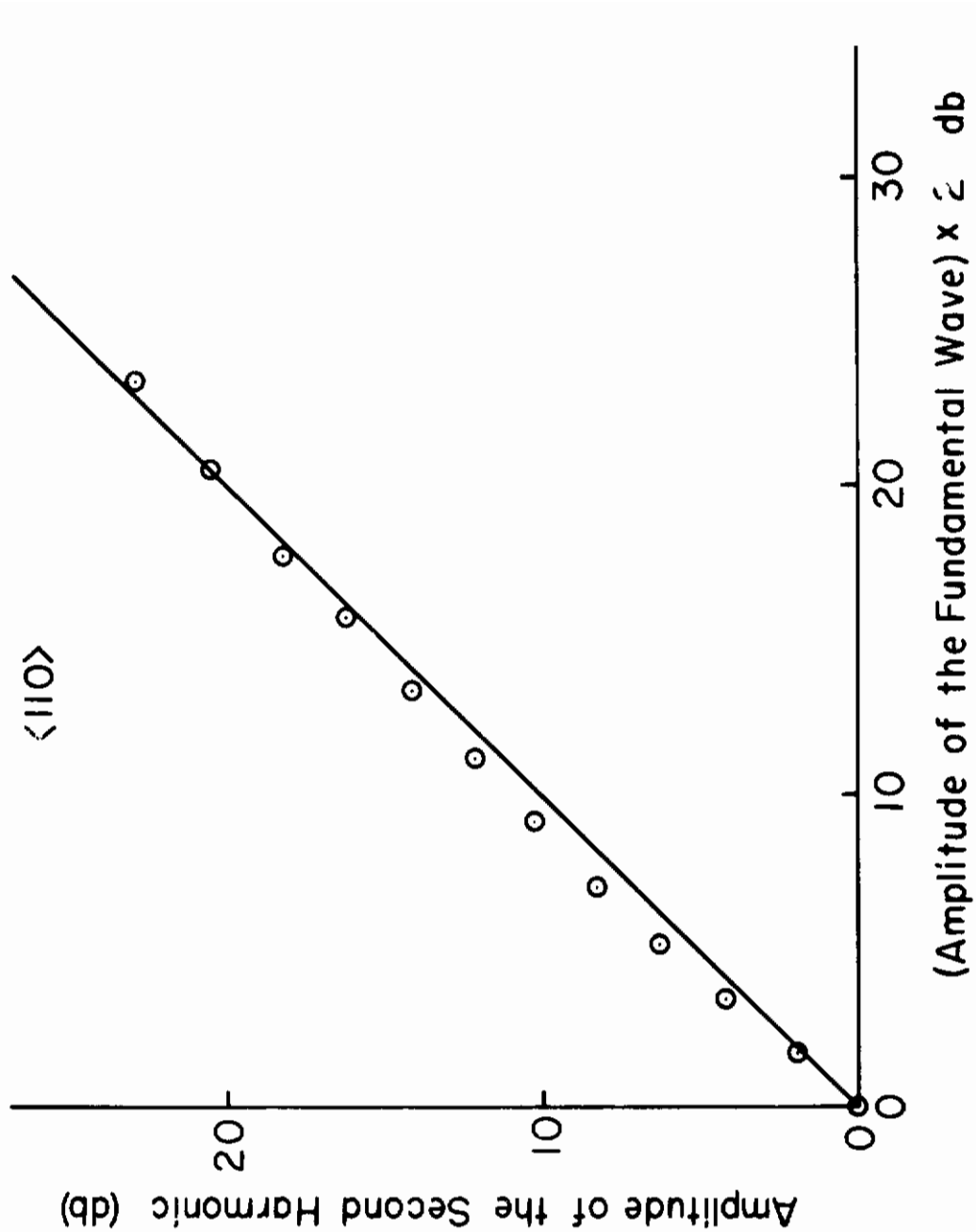

Figure 6. Amplitude of the Second Harmonic as a Function of the Amplitude of the Fundamental Wave. Aluminum Single Crystal, <110> Orientation.

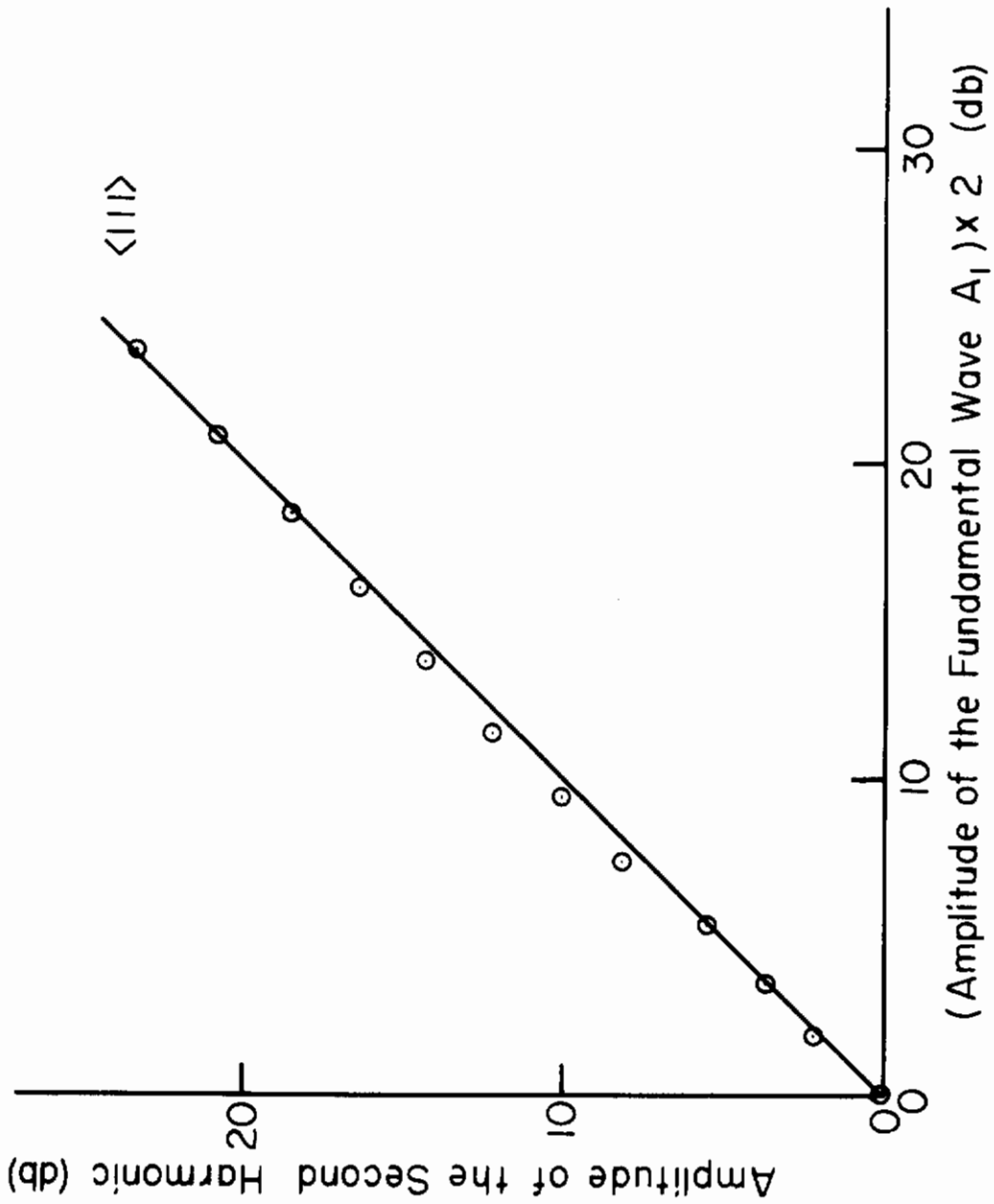

Figure 7. Amplitude of the Second Harmonic as a Function of the Amplitude of the Fundamental Wave. Aluminum Single Crystal, <111> Orientation.

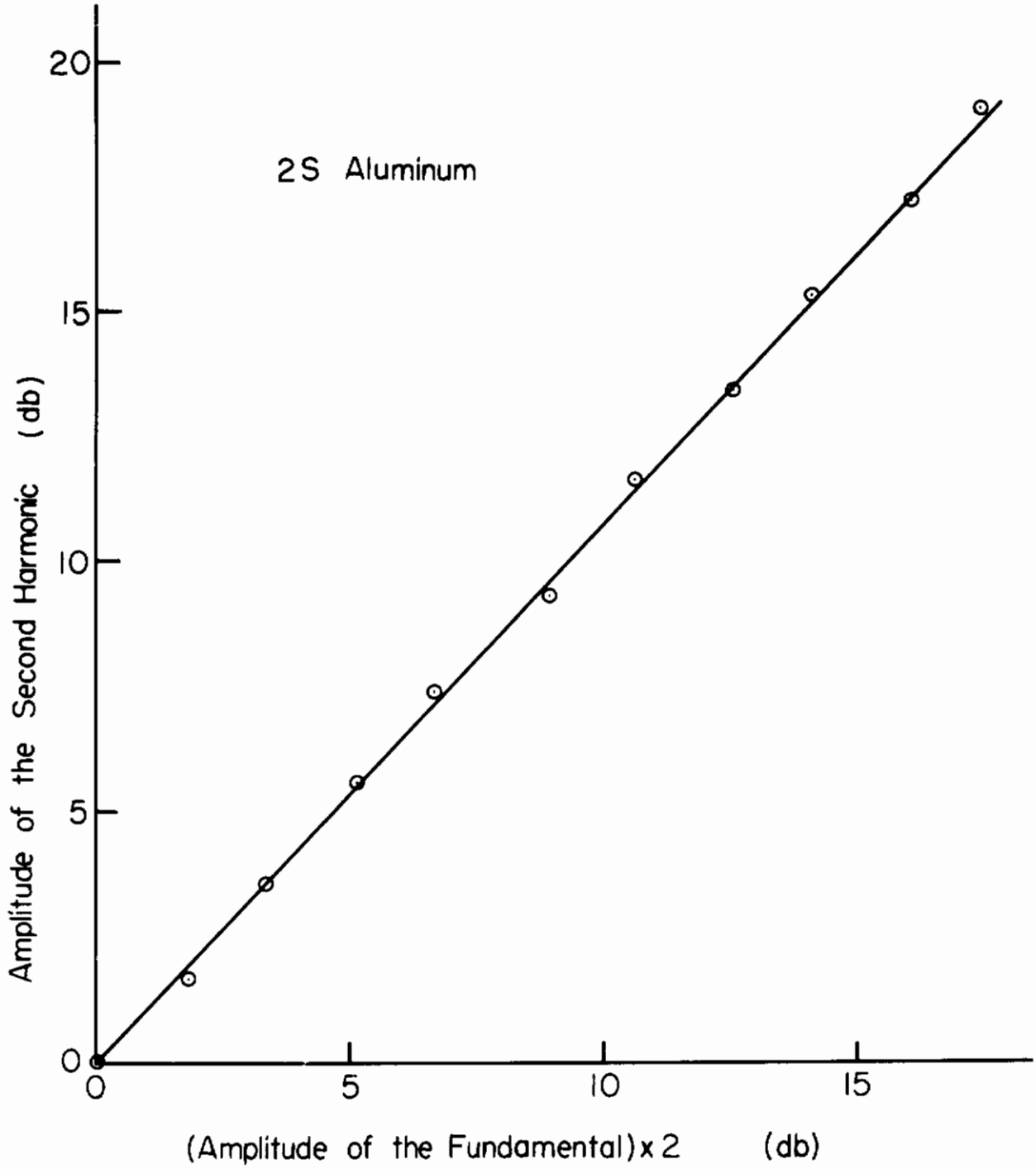

Figure 8. Amplitude of the Second Harmonic as a Function of the Amplitude of the Fundamental Wave. 2S Aluminum.

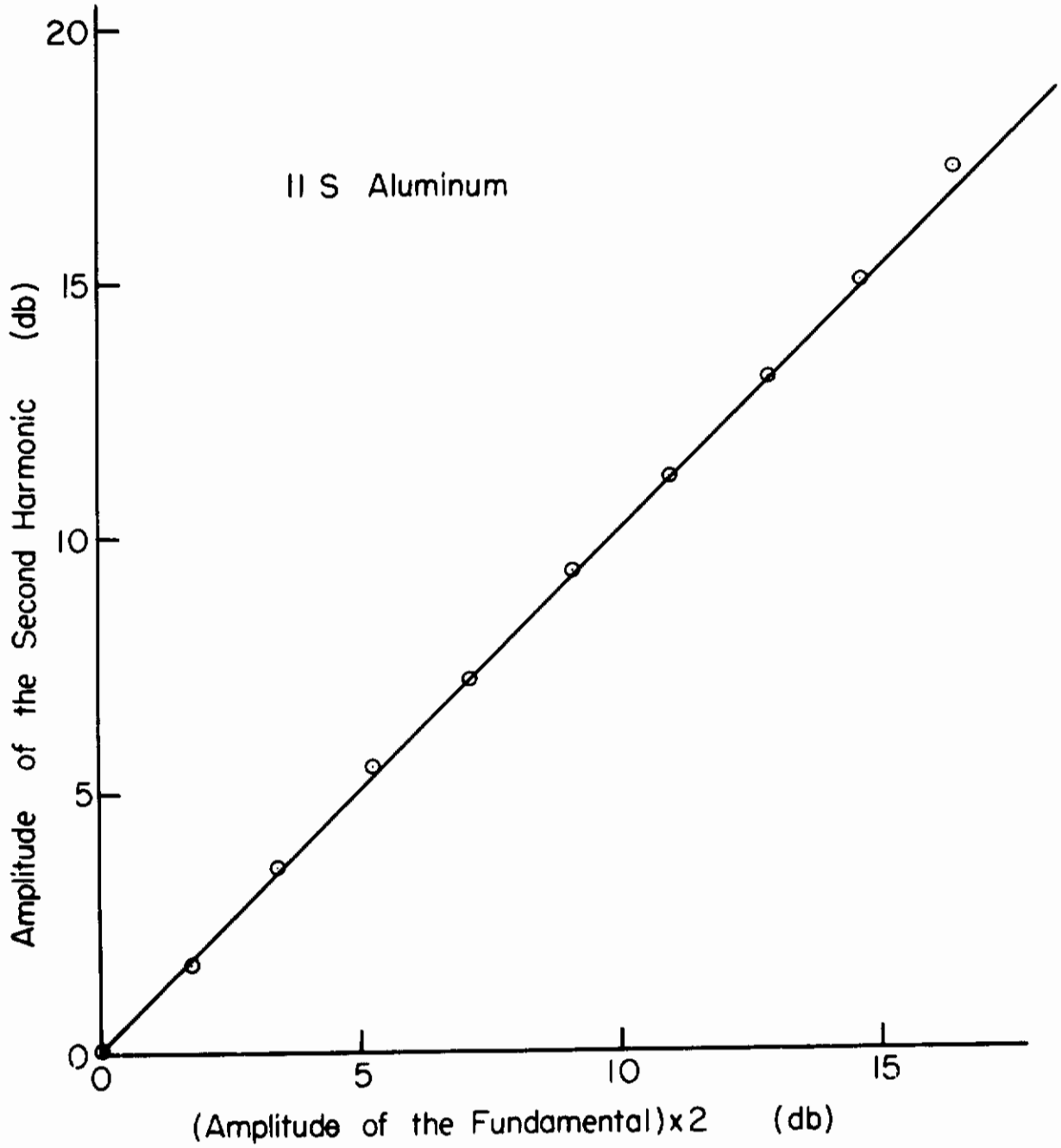

Figure 9. Amplitude of the Second Harmonic as a Function of the Amplitude of the Fundamental Wave. 11S Aluminum.

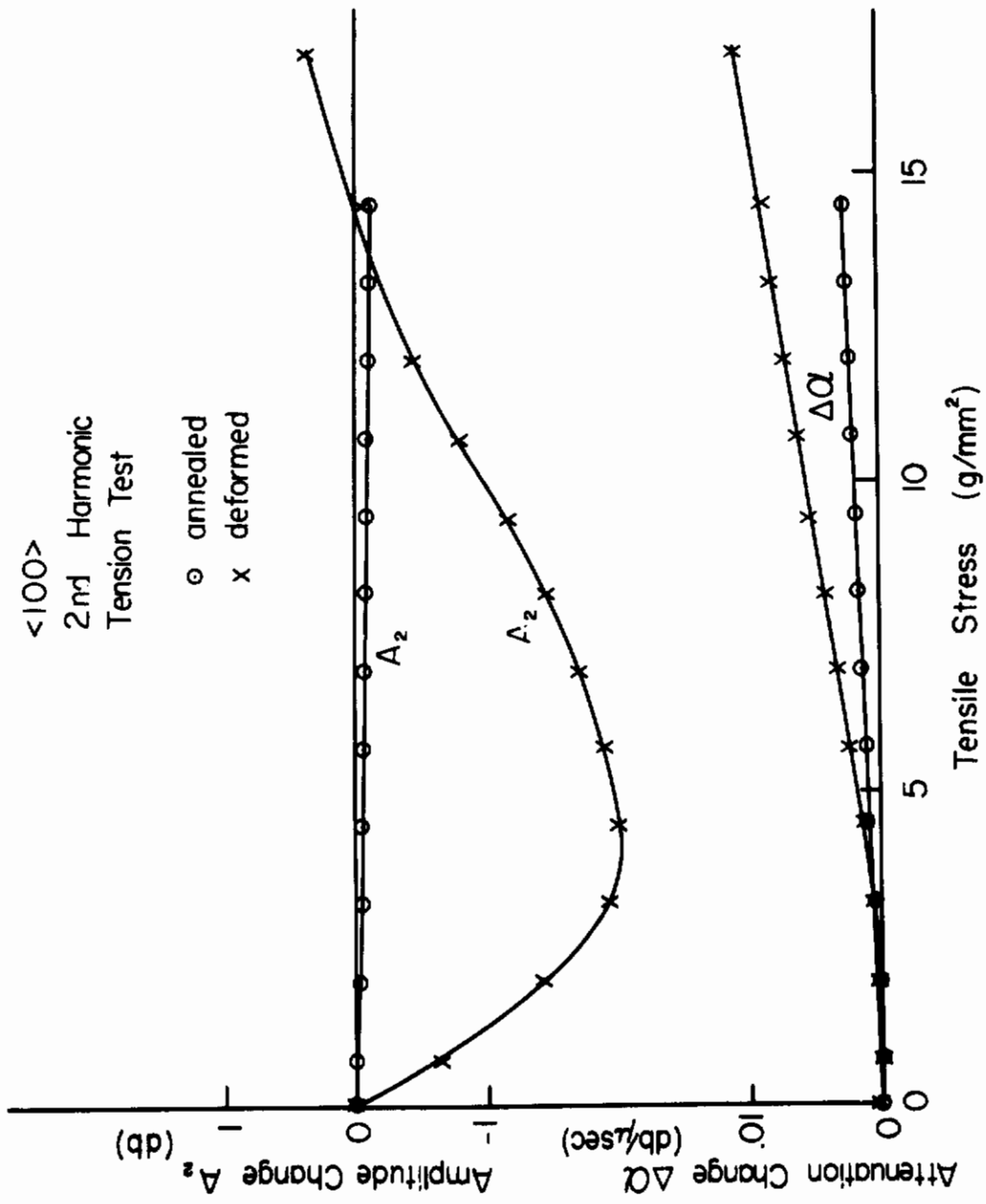

Figure 10. Effect of Plastic Deformation on the Amplitude of the Second Harmonic and the Attenuation of the Fundamental Wave, as a Function of Bias Stress in Tension. Aluminum Single Crystal, <100> Orientation.

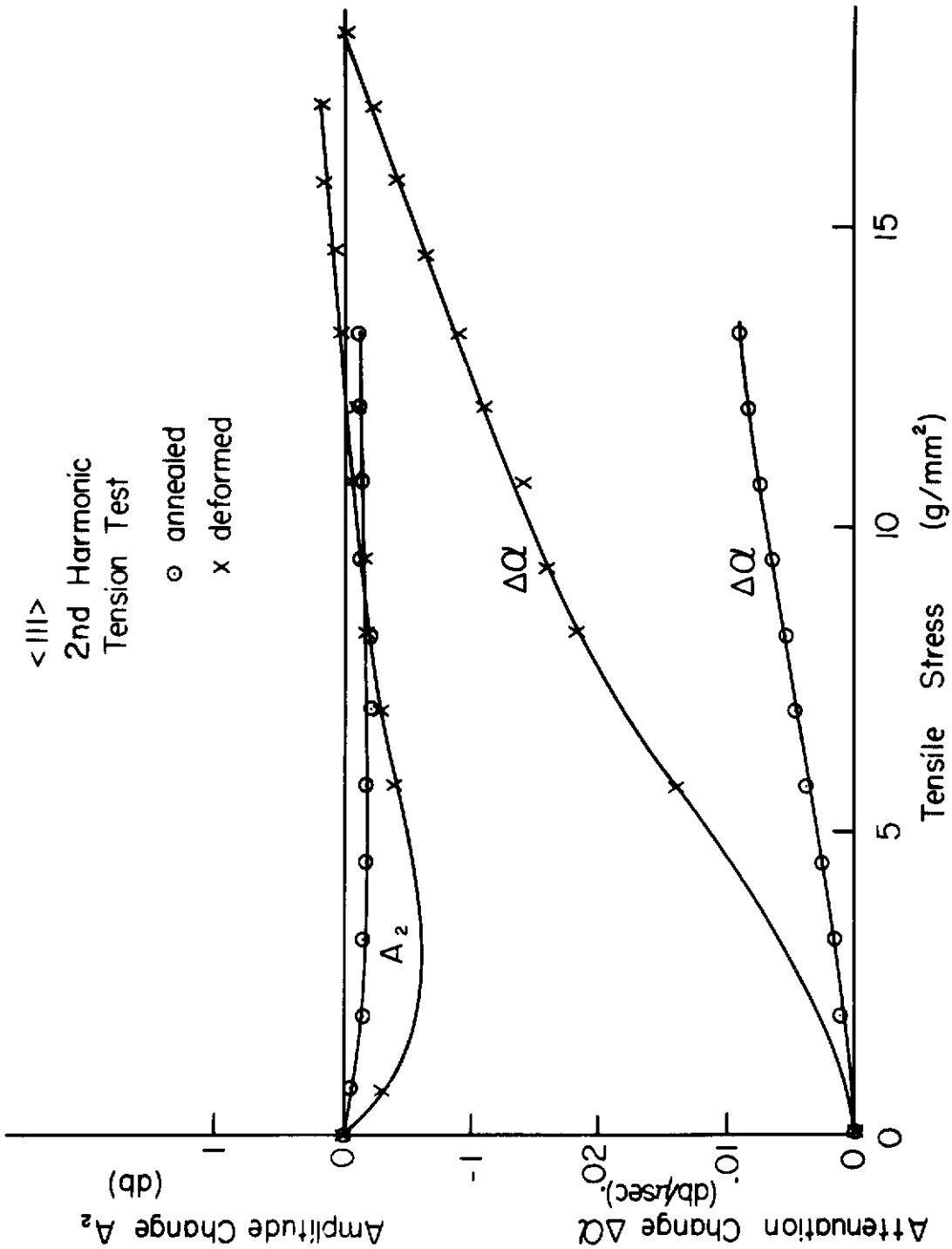

Figure 11. Effect of Plastic Deformation on the Amplitude of the Second Harmonic and the Attenuation of the Fundamental Wave, as a Function of the Bias Stress in Tension. Aluminum Single Crystal, <111> Orientation.

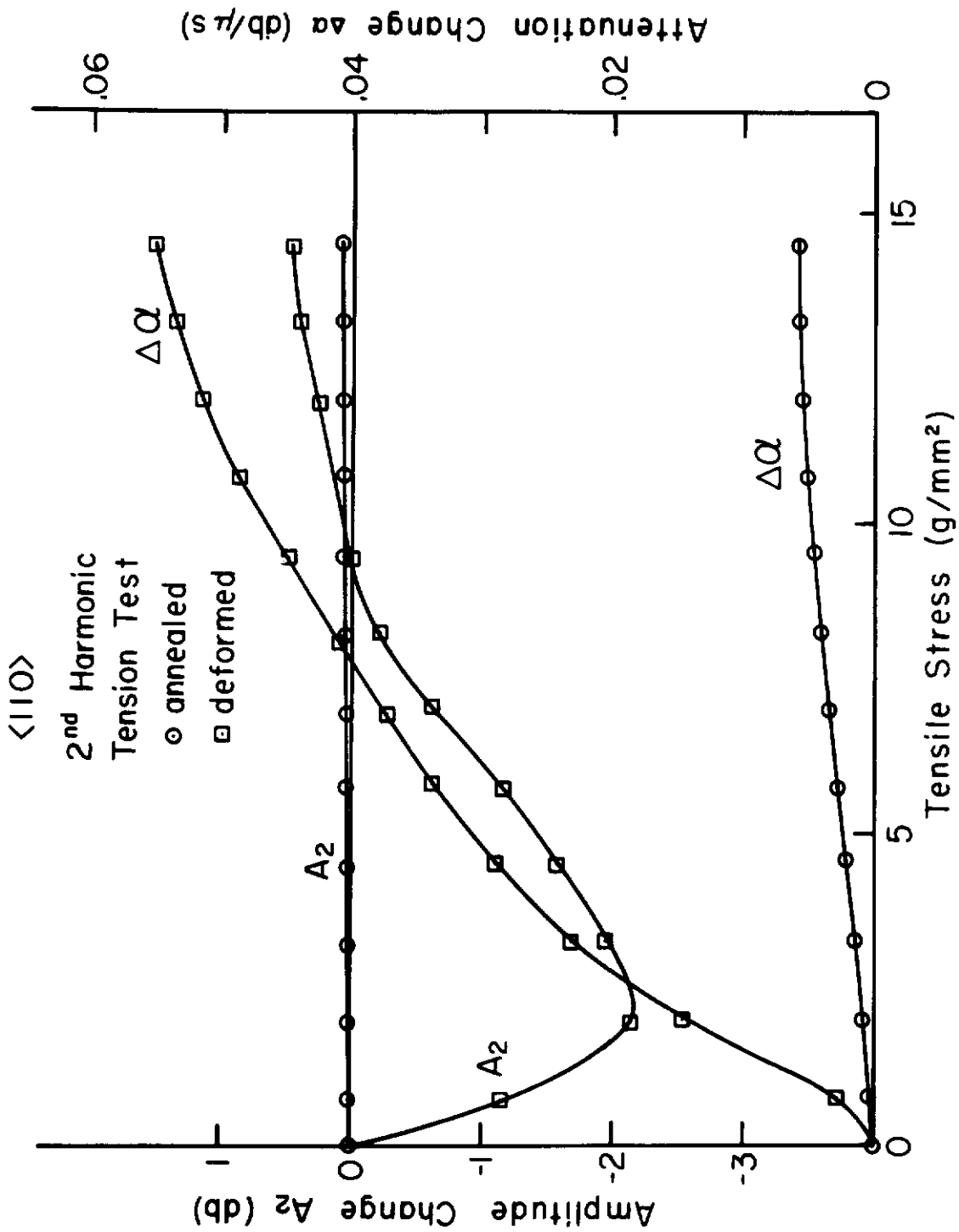

Figure 12. Effect of Plastic Deformation on the Amplitude of the Second Harmonic and the Attenuation of the Fundamental Wave, as a Function of Bias Stress in Tension. Aluminum Single Crystal, <110> Orientation.

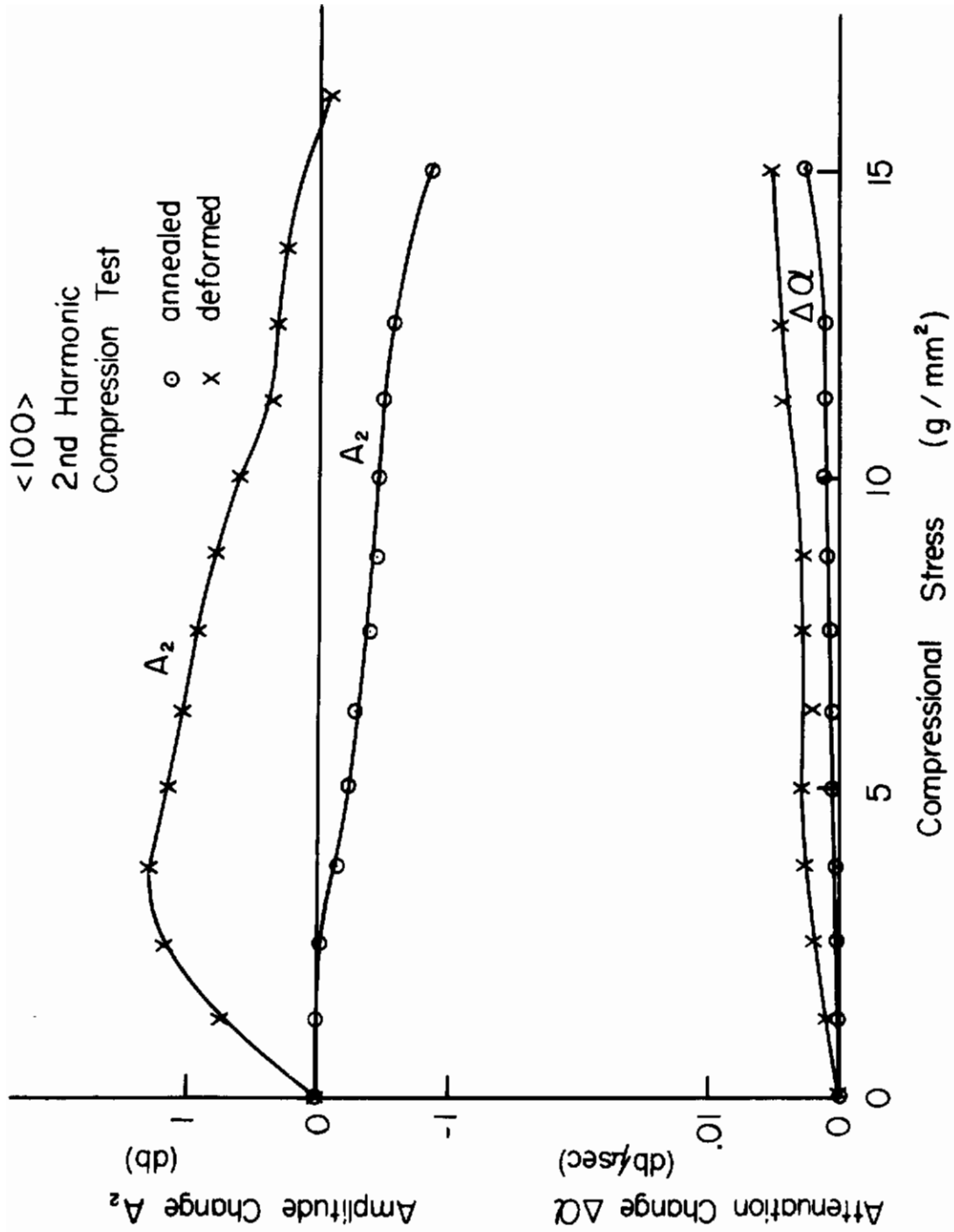

Figure 13. Effect of Plastic Deformation on the Amplitude of the Second Harmonic and the Amplitude of the Fundamental Wave, as a Function of Bias Stress in Compression. Aluminum Single Crystal, <100> Orientation.

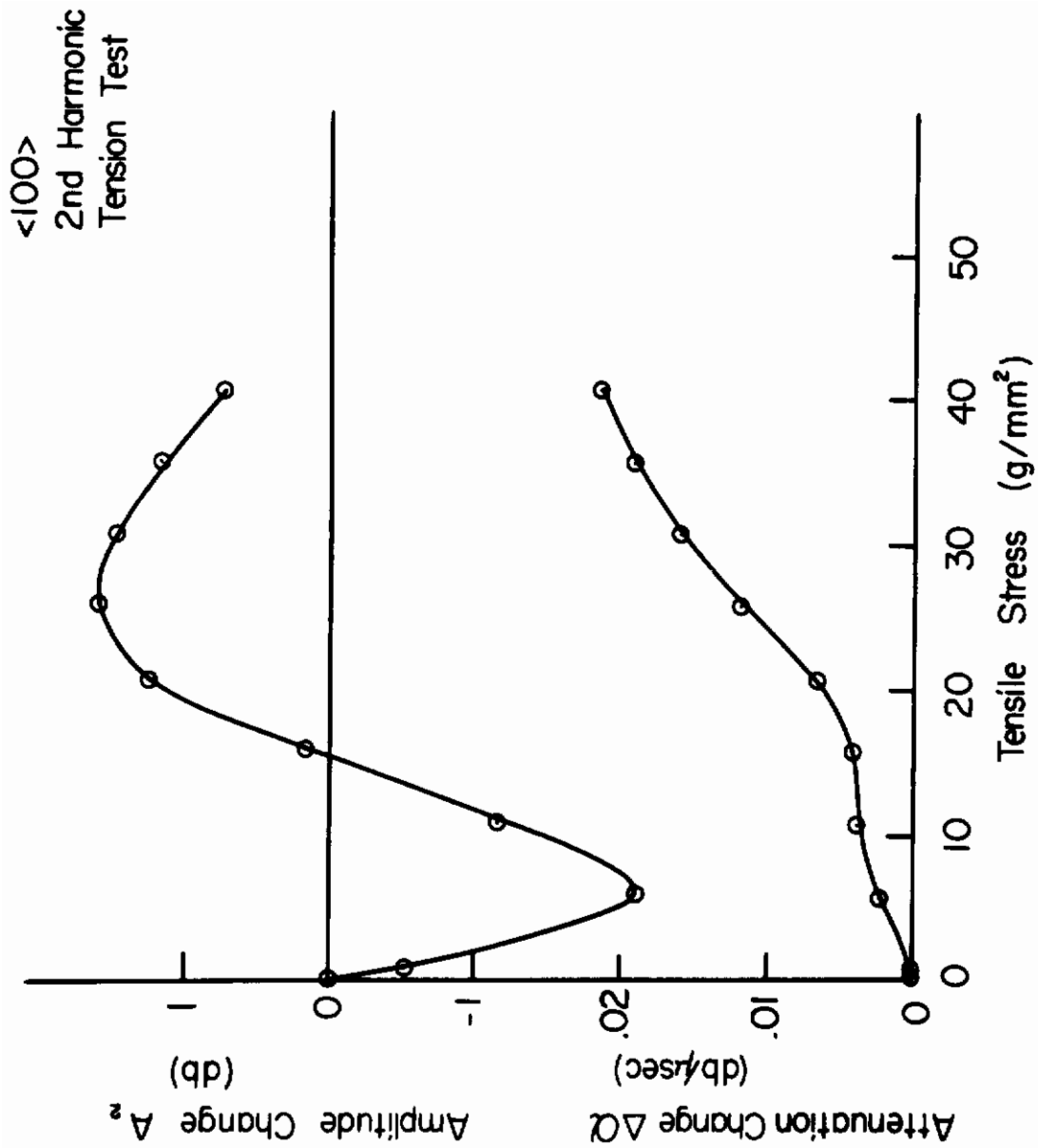

Figure 14. Effect of Larger Bias Stress.
(The same Specimen shown in Figure 10).

examined as a function of the amplitude. A calibrated stepped attenuator was used to adjust pulse amplitude without distortion. The results in the case of <110> orientation are shown in Figure 15. An increase in the attenuation was detected as the amplitude of the wave increased, and the amount of the increase was considerably larger after the specimen had been plastically deformed.

Orientation Dependence

In the case of aluminum single crystals (face centered cubic structure), there are twelve slip systems ({111} plane and <110> direction). For <100> orientation, eight out of the twelve slip systems are equally stressed, for <111> orientation six slip systems and for <110> orientation four slip systems are equally stressed. On the other hand, the resolved shear factors for each slip plane for a tensile stress are 0.408, 0.272 and 0.408 respectively. Thus, the combination of the number of slip systems and the corresponding resolved shear factor gives the relative sensitivity factors (for a uniaxial stress) 1:0.5 :0.5 for <100>, <110> and <111> orientations respectively. For the attenuation change, the above consideration is true only when the deformation is small so that the dislocations in the slip systems do not intersect each other. Since the attenuation is proportional to the fourth power of the dislocation loop length, the attenuation increase due to an applied external stress will slow down as soon as dislocation intersections take place. Therefore, the attenuation change is expected to be largest in the <110> orientation and smallest in the <100> orientation, with intermediate values in the <111> orientation. This effect was investigated in detail and reported previously. (8) In the stress region where the dislocation intersections do not take place appreciably, the amount of the second harmonic generated by dislocations should be proportional to the orientation factor, i.e. larger in the <100> orientation and smaller and nearly equal in the <110> and <111> orientations.

In order to check this prediction, annealed specimens of <100>, <111>, <110> orientations were stressed in tension. The results are shown in Figure 16. Both attenuation changes of the fundamental wave and amplitude changes of the second harmonic confirm the above prediction.

(8) A. Hikata, B. Chick, C. Elbaum and R. Truell; Acta Met., 10, 423 (1962)

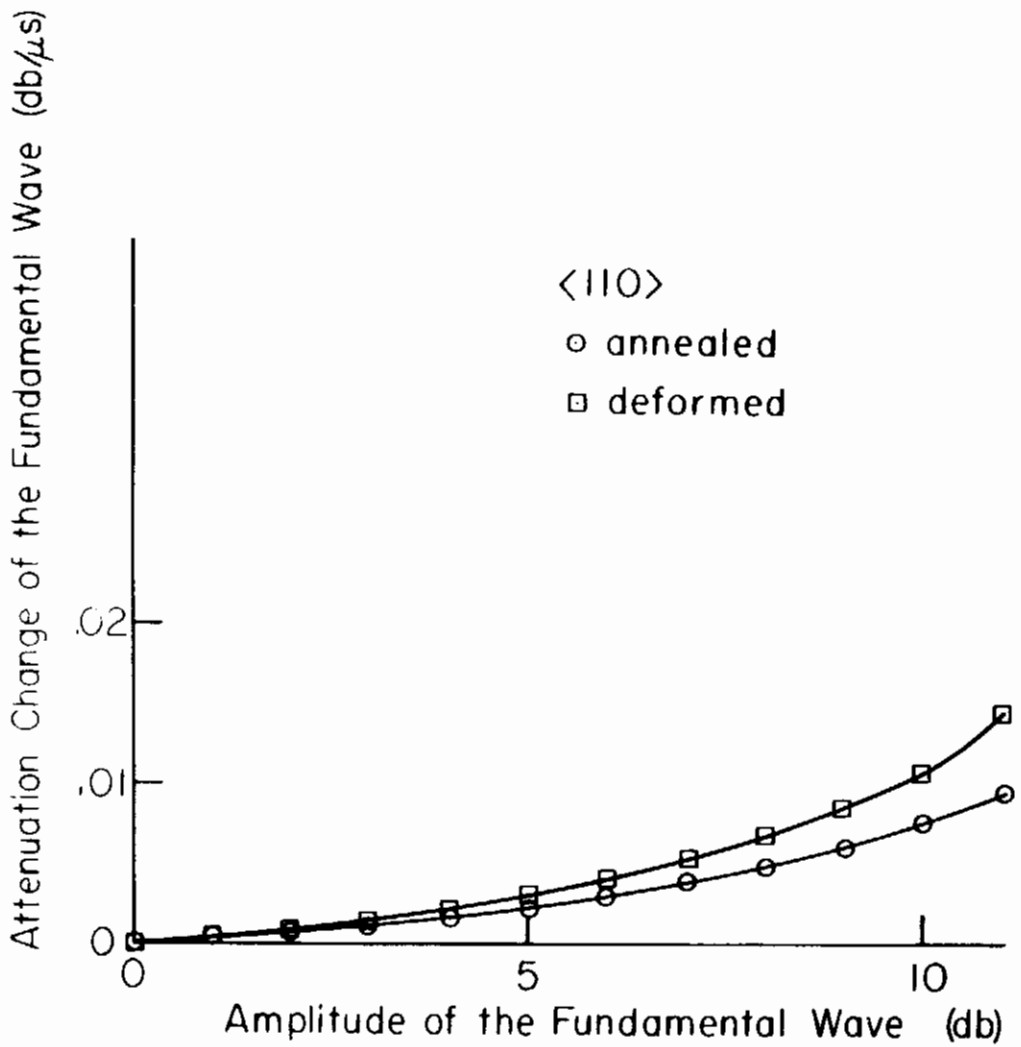

Figure 15. Effect of Plastic Deformation on the Attenuation Change of the Fundamental Wave as a Function of the Amplitude.

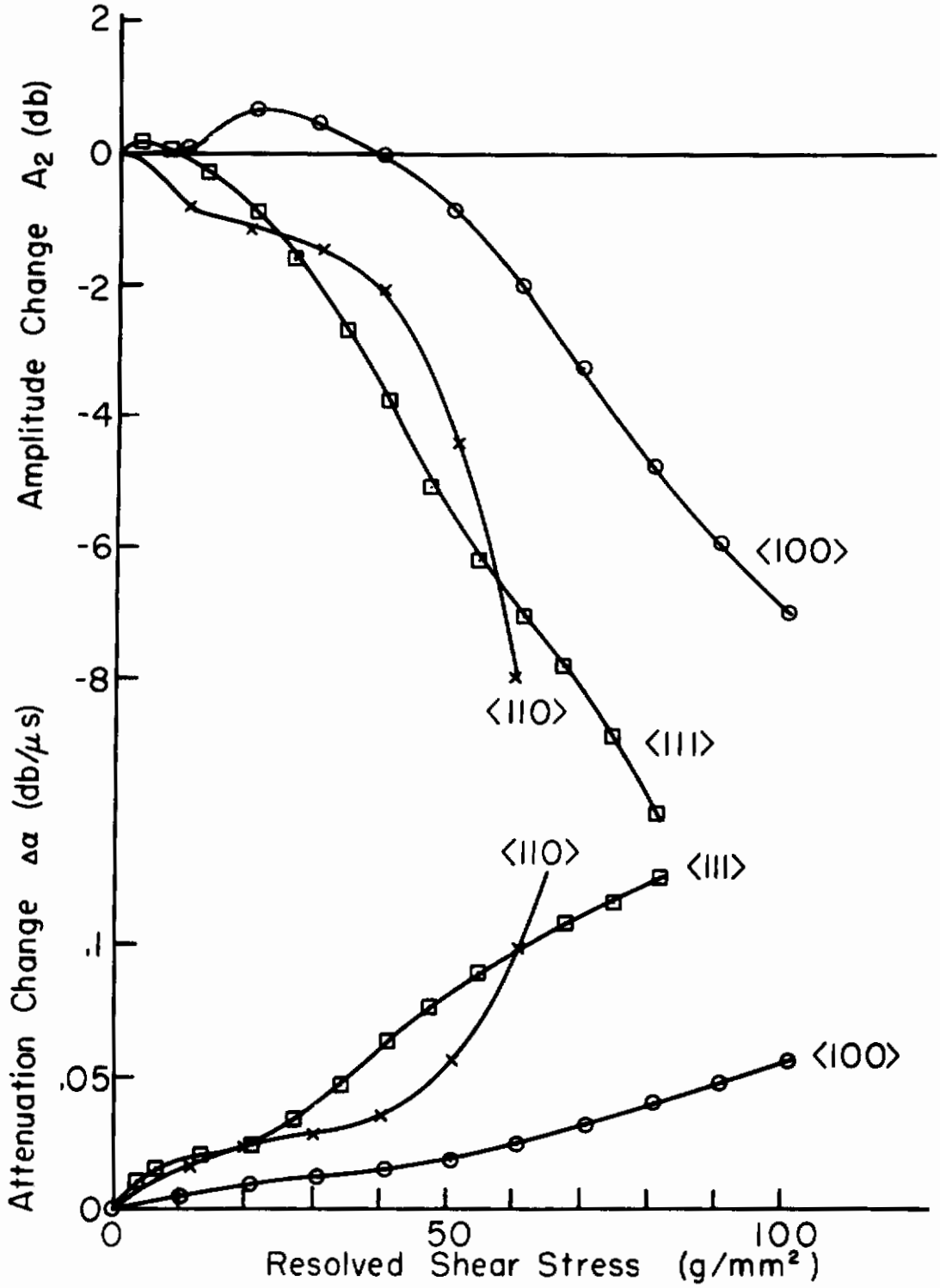

Figure 16. Orientation Dependence of the Amplitude of the Second Harmonic as a Function of Bias Stress, and the Corresponding Attenuation Change of the Fundamental Wave.

SUMMARY

The experiments and the associated theory discussed show clearly that dislocations contribute to the anharmonic behavior of crystals. This contribution is measured through the changes as a function of stress, in the amplitude of the second harmonic of a fundamental wave propagating in the crystal.

In the case of single crystals the amplitude of the second harmonic changes vary markedly with stresses ranging from zero to 10^6 dynes/cm^2. In alloys, there are essentially no changes of that amplitude even for stresses up to 10^7dynes/cm^2. These observations are consistent with the predicted dependence of the amplitude on dislocation loop length and on the static stress. Small amounts of plastic deformation (in the case of single crystals) increase the effect in qualitative agreement with the predicted dependence on dislocation density.

The effect of crystal orientation was checked for three cases, namely $<100>$, $<110>$, $<111>$; here again the effect was found to follow the order predicted by the theoretical considerations.

II. Studies of Defects in Alkali Halides

Lithium fluoride

Simultaneous investigations of ultrasonic attenuation changes and of electrical conductivity changes have been undertaken for the purpose of studying the kinetics of point defect interactions with dislocations. Alkali halides are particularly suited for this study, because their electrical conductivity is of the ionic type and gives a direct measure of the number of mobile point defects in the solid. At the same time, the changes in dislocation damping provide information on the number of point defects that reach the dislocations in a given time. Lithium fluoride was chosen for this study, because of larger values of conductivity near room temperature than in the case of sodium chloride, which was used in all the previous investigations. This feature allowed us to extend the measurements over a wider temperature range (near room temperature) where our ultrasonic techniques are also applicable.

In this study it is important to cover as wide a temperature range as possible for the following reasons. The temperature dependence of the conductivity is known and is associated (in the temperature range considered) with the diffusion of positive ion (single) vacancies. A comparison of the temperature dependence of attenuation recovery with the above would, therefore, give a direct indication of whether the recovery process is associated with the migration of single vacancies. Preliminary experiments have been carried out on the measurement of ultrasonic attenuation and electrical conductivity as a function of plastic deformation in lithium fluoride. The samples of lithium fluoride used are 3" x 1/4" x 1/4" and they are pulled in tension in an Instron testing machine in much the same way as in our experiments with sodium chloride samples reported previously (9).

Difficulties have been encountered in gluing the sample into the grips of the testing machine, especially in connection with tests at higher temperatures. However, a technique has been found to hold the sample satisfactorily for tension tests up to at least 190°C.

A special hot-cold chamber has been used and the ultrasonic attenuation was measured at a frequency of 60 mc/sec. Stress-strain measurements, attenuation-strain measurements and conductivity-strain measurements have been obtained during deformation as shown in Figure 17 . The sharp increase in attenuation and in conductivity coincide with one another and with the onset of macroscopic plastic deformation. These results are consistent with the idea that plastic deformation increases the dislocation density as well as the number of vacancies. The increased number of vacancies is reflected by the change in electrical conductivity in ionic crystals at a given temperature.

Recovery of conductivity as a function of time following fracture of the specimen at 190°C is shown in Figure 18. The shape of this curve for the recovery of conductivity is obviously quite different from the type of curve for changes in attenuation following deformation in metals. Because of the sensitive relation of the attenuation to the mechanism of pinning of dislocations by point defects, the attenuation recovery curve usually shows a rapid decrease at the beginning of

(9) A. Hikata, B. Chick, C. Elbaum and R. Truell; Applied Physics Letters, 2, 5 (1963)

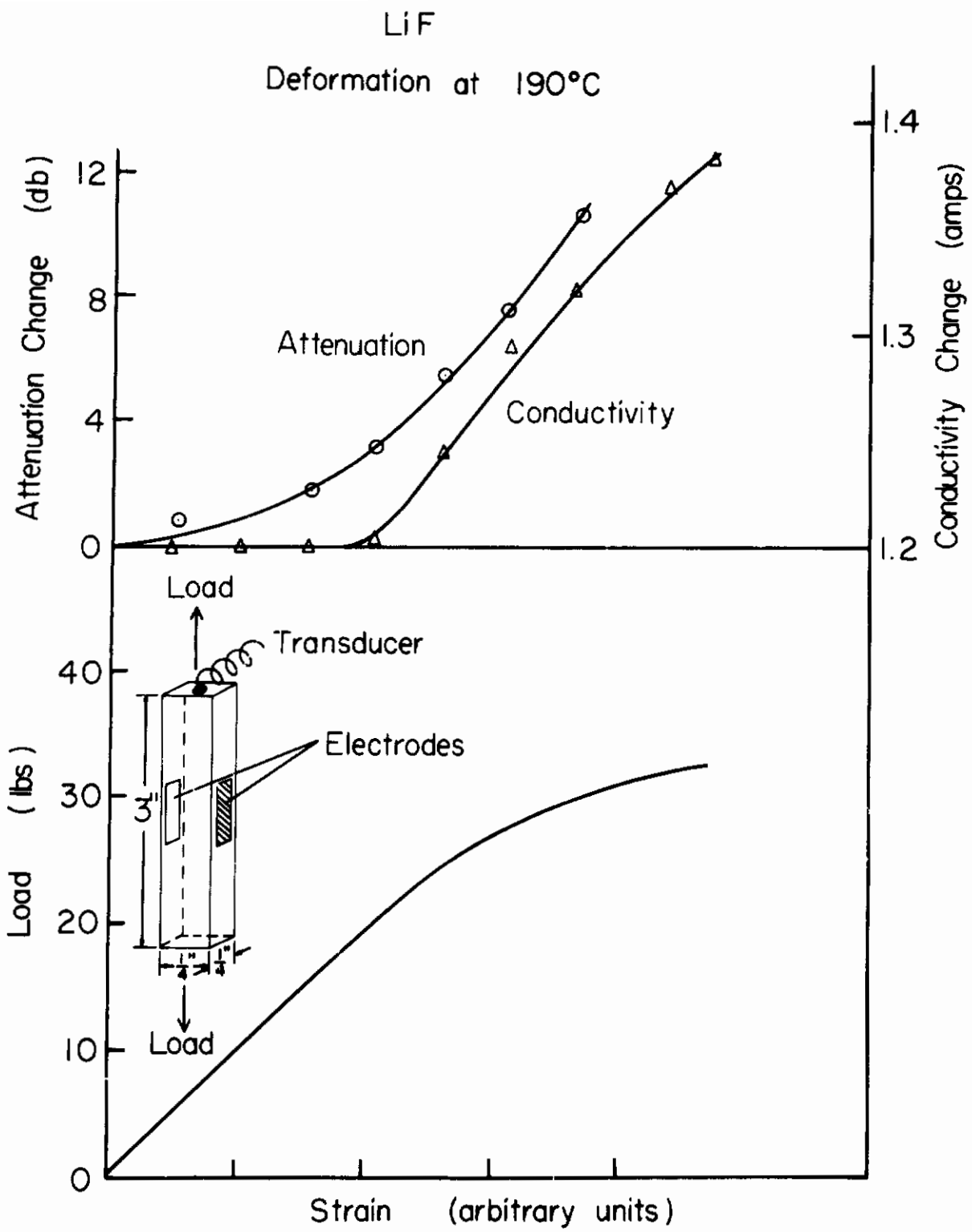

Figure 17. Load Attenuation Change and Conductivity Change of Lithium Fluoride Single Crystal as a Function of Strain at 190°C. Sizes of the Specimen and the Experimental Arrangement are also Shown Schematically.

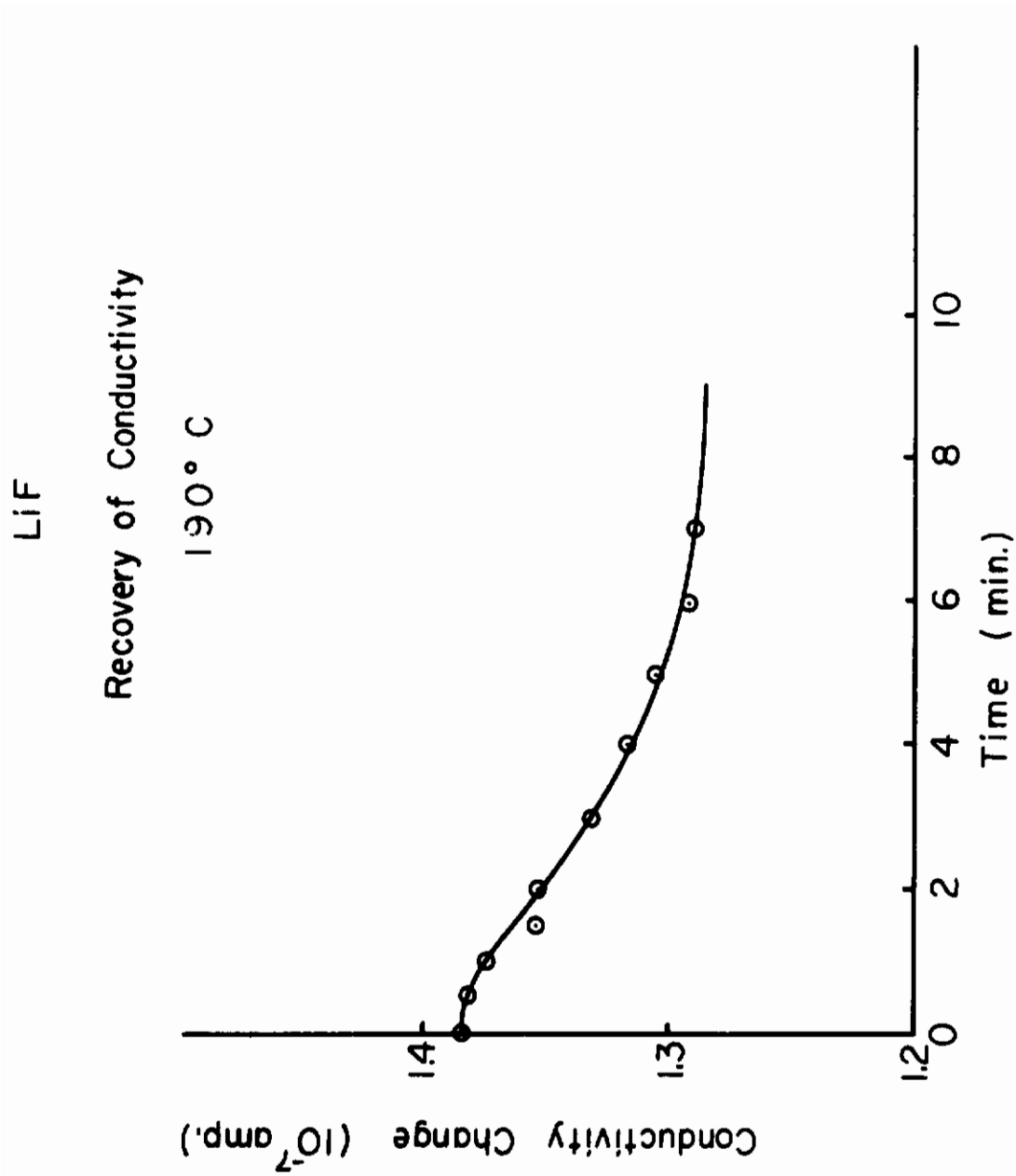

Figure 18. Recovery Conductivity Change of Lithium Fluoride Crystal at 190°C after Deformation.

recovery. On the other hand conductivity in lithium fluoride is proportional to the number of positive ion vacancies remaining in the crystal after deformation. Consequently, there should be a period at the beginning of the conductivity recovery where no appreciable change in conductivity appears. Attenuation recovery and electrical resistivity recovery are obviously quite different in ionic crystals.

Unfortunately the lithium fluoride specimen fractured before the tensile machine was stopped. Consequently attenuation recovery could not be measured and a direct comparison between attenuation recovery and conductivity recovery was not obtained at this temperature in this particular experiment.

Sodium chloride

An electrical charge is expected to form on external surfaces and on dislocations in alkali halides because of differences in the free energies of formation of positive and negative ion vacancies. A difference of potential between an external surface and the interior of a crystal, or between a dislocation and its surroundings is thus developed. This problem has been explored during the previous year by means of plastic deformation experiments (10).

Another approach to the problem of charge behavior and dislocations had been undertaken, and explored during the period covered by this report. In view of the differences in the free energies of formation and in the mobilities of the two types of vacancies, it is expected that a difference of potential should develop between the cooler and hotter ends of a crystal placed in a temperature gradient. From the value of the potential difference for a given average temperature and given temperature gradient it should be possible, in principle, to deduce the values of the parameters that govern charge accumulation. An experiment has been designed and preliminary tests have been carried out to check the above hypothesis.

A sodium chloride single crystal about 1 inch long was placed at the edge of a furnace so that when the temperature of the furnace was raised, a thermal gradient across the specimen was established. Electrodes, one on the hotter end and one on the cooler end of the specimen, were connected to an electrometer and a potentiometer to measure the accumulated charge and the potential difference across the sample. Since the charge carriers in sodium chloride are predominantly positive ion vacancies, the current J is determined by thermal diffusion $A\cdot(\partial T/\partial x)$ and concentration diffusion $B\cdot(\partial C/\partial x)$ where $\partial T/\partial x$ is the temperature gradient and $\partial C/\partial x$ is the concentration gradient of positive ion vacancies.

A and B are considered to be constants, thus

$$J = A \frac{\partial T}{\partial x} - B \frac{\partial C}{\partial x} .$$

The sign of the current J, or the potential difference, depends on the relative sizes of the two terms. This relation together with experiments would, it was hoped, clarify the mechanism as well as the size of the charge developed on the surface of a sodium chloride crystal. It is hoped that if this can be done the results may be extended to the case of dislocations within the crystal since the dislocations also act as sources and sinks for vacancies.

(10) A. Hikata, C. Elbaum, B. Chick and R. Truell; Journal of Applied Physics 34, 2154, (1963).

We have performed several experiments of the electrical potential differences across the ends of a sodium chloride crystal as a function of the imposed temperature gradient. Figure 19 shows the measured temperatures of the hotter (T_1) and cooler (T_2) ends of the sample during the time in which the temperature was raised and lowered during one heating cycle. Figure 20 shows the potential difference across the ends of the sample during the heating cycle. It is clear that this electrical potential difference reverses sign several times as the thermal gradient increases. These reversals cannot be accounted for in terms of the convential theory of thermal diffusion. According to the ideas mentioned above we attribute these reversals to the charge accumulation at the external surfaces, and a more detailed analysis involving this effect is in progress.

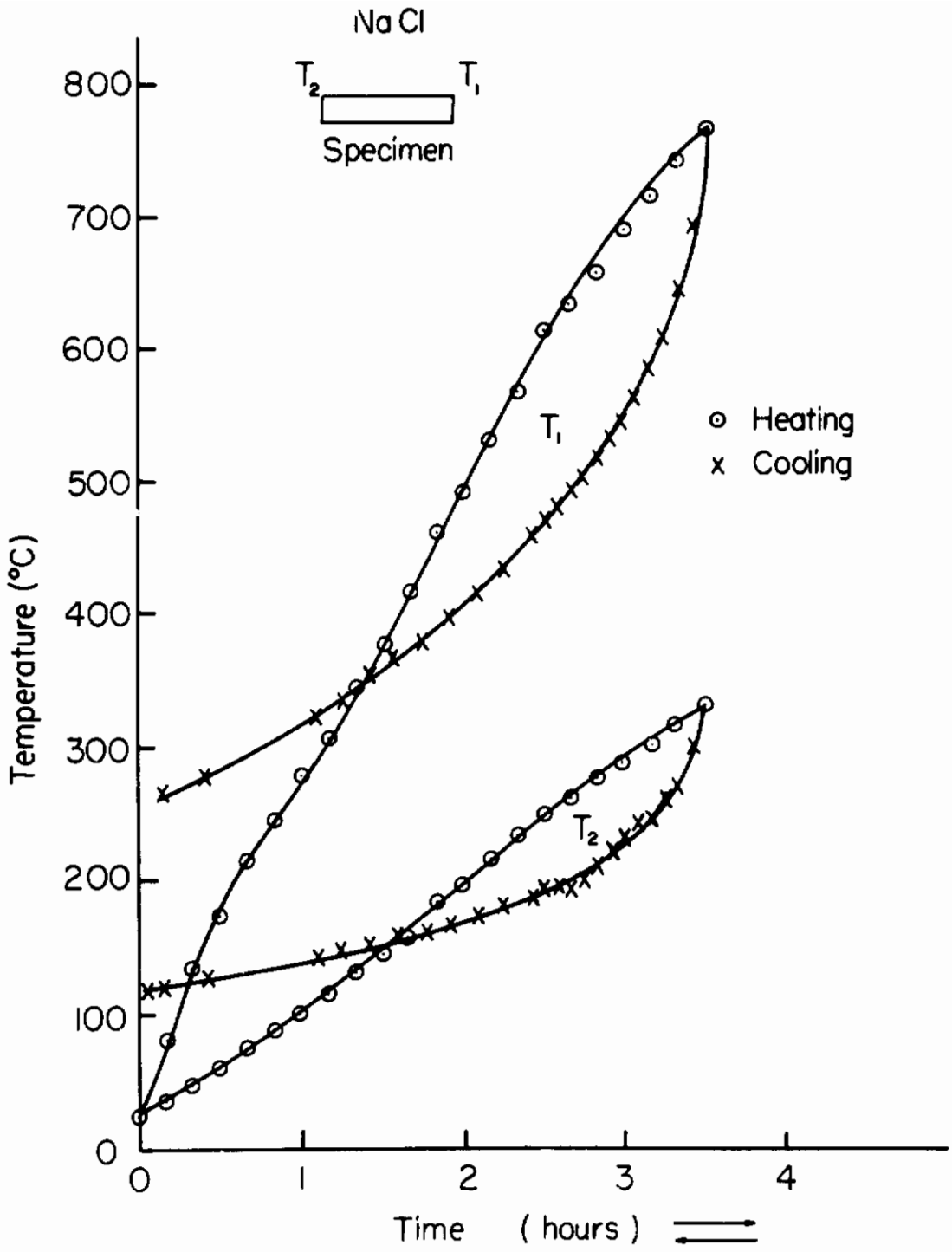

Figure 19. Temperature of the Hotter (T_1) and the Cooler (T_2) Ends of the Sodium Chloride Specimen During the Heating Cycle.

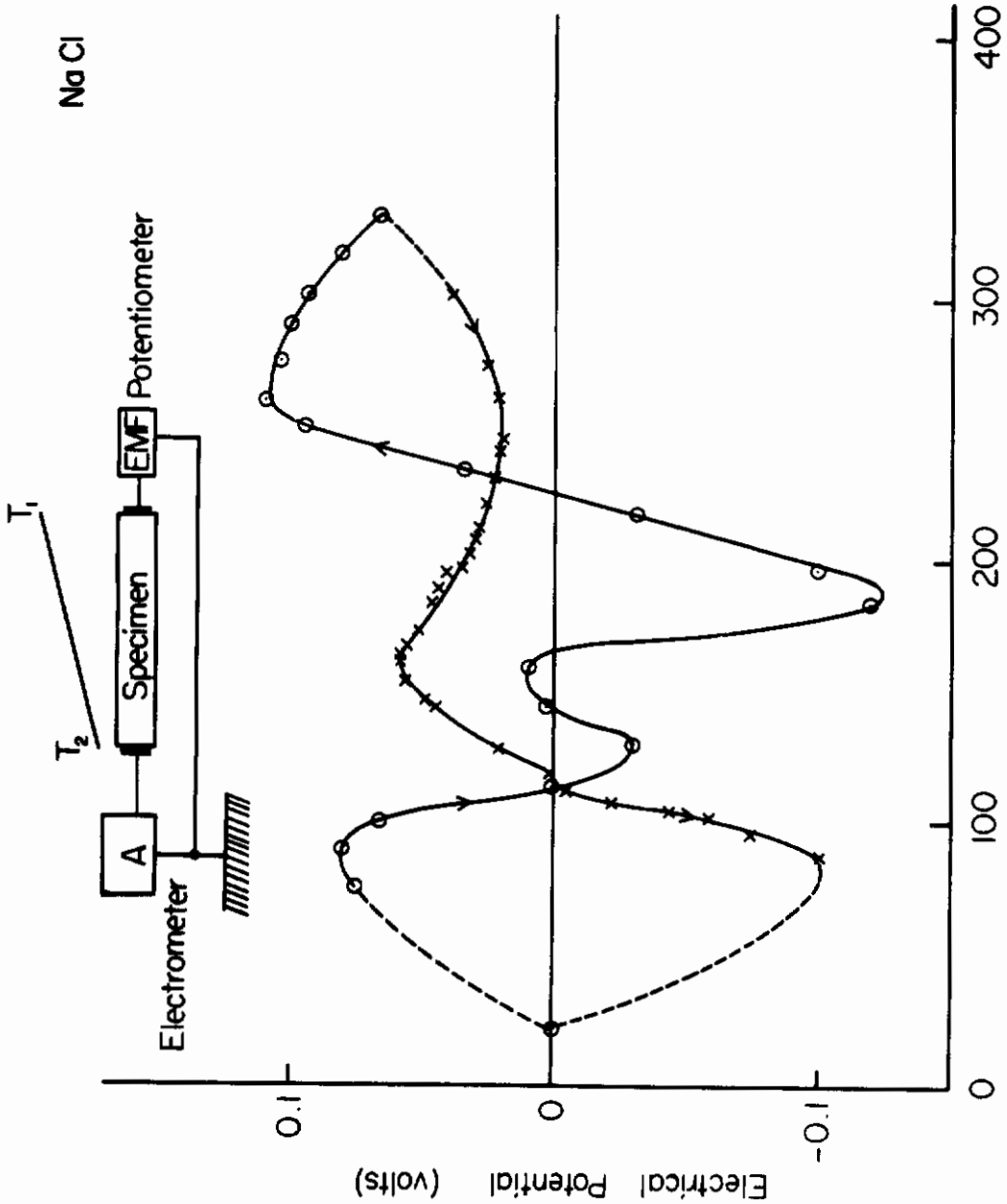

Figure 20. Electrical Potential Difference Across the Specimen During the Heating Cycle. Experimental Arrangement is also Shown Schematically.

III. Interactions Between Point Defects and Dislocations

Recovery of attenuation

Dislocation damping theory shows that the attenuation α and fractional velocity change $\Delta G/G_o$ depend on loop length (average)L and dislocation density Λ in the following way

$$\alpha = K_1 \Lambda \frac{1}{(X^2 - 1)^2 + Y^2} \tag{18}$$

$$\frac{\Delta G}{G_o} = K_2 \Lambda \frac{(1-X^2)}{(X^2 - 1)^2 + Y^2} \tag{19}$$

where $X = \frac{\omega_o}{\omega}$, $Y = \frac{d}{\omega}$, ω_o (resonant frequency) $= \frac{\pi}{L}(\frac{C}{A})^{1/2}$

$d = \frac{B}{A}$, ω(angular frequency at which the measurements are taken)

K_1 and K_2 are constants, B is the damping force per unit length, C is an effective tension in a bowed out dislocation and A is the effective mass per unit length.

It has been found that plastic deformation changes the attenuation and the apparent elastic modulus of a crystalline material through the factors Λ and L in the above expressions. Following the deformation, these quantities recover toward their original values. To date, three mechanisms have been put forward in order to explain this kind of recovery phenomena; 1) annihilation theory (disappearance of dislocations by cancelling out each other or escaping from the specimen), 2) rearrangement theory (immobilization of dislocations against the applied oscillatory stress by interaction of the dislocations with other dislocations), 3) pinning theory (immobilization by interactions of the dislocations with point defects, such as vacancies). However, on the basis of the view point discussed in our earlier paper (11), we believe that the predominant mechanism for the recovery in our experiments is the pinning mechanism, and what follows is the modification of the analysis proposed in that paper. When polycrystalline materials are used, or when the amount of plastic deformation induced prior to the recovery experiments is large, the resonant frequency ω_o determined by dislocation loop length L becomes large enough compared with the working frequency ω, so that the term Y^2 can be neglected compared with the term $(X^2-1)^2$ in the expressions (18) and (19) (low frequency approximation). In such a case, the expression for the normalized recovery curves of attenuation and velocity change can be written in the following way

$$\alpha_n = \frac{1}{[1 + (\beta t)^{2/3}]^4} \tag{20}$$

where $\alpha_n = \frac{\alpha}{\alpha_o}$ and α_o is the attenuation value immediately after deformation but before recovery i.e. value of α at $t = 0$.

$$(\frac{\Delta G}{G_o})_n = \frac{1}{[1 + (\beta t)^{2/3}]^2}, \tag{21}$$

where $\beta = K_3 \frac{JD}{kT}$,

(11) A. Granato, A. Hikata and K. Lucke, Acta Met. 6, 470 (1958).

D is the diffusion coefficient of point defects responsible for the pinning, J is a parameter measuring the strength of the Cottrell attraction, t is the recovery time, KT has the usual meaning and K_3 is a constant. In deriving the above expressions it is assumed that the point defects migrating toward dislocations obey Cottrell-Bilby's $t^{2/3}$ law. The validity of this $t^{2/3}$ law for the attenuation recovery is not established, and it remains to be investigated with specifically designed experiments. Nevertheless, the expressions (20) and (21) were rather successful in describing the results obtained in the earlier experiments (polycrystalline materials and plastic deformation over one per cent). As shown in the final reports for 1961 and 1962, when the deformation is limited to small values, an anomalous effect is observed. This anomalous effect shows how under special conditions an increase of loop length L due to unpinning by applied atress, results in an increase in the velocity of the ultrasonic waves while the attenuation increases (a physical explanation of the velocity anomaly is given in the last annual report (1962) (12). In such an overdamped case, the term Y^2 is not negligible compared with the term $(x^2 - 1)^2$, and the expression (20) and (21) are no longer applicable. Expressions of normalized recovery curves for attenuation and velocity change in the overdamped case can be derived from (18) and (19), assuming the same $t^{2/3}$ law

$$\alpha_n = \frac{\alpha}{\alpha_o} = \frac{(X_o^2 - 1)^2 + Y^2}{\left[X_o^2 \left\{1 + (\beta t)^{2/3}\right\}^2 - 1\right]^2 + Y^2} \qquad (22)$$

$$\left(\frac{\Delta G}{G_o}\right)_n = \frac{\Delta G}{G \cdot K_4} = \frac{1 - X_o^2 \left\{1 + (\beta t)^{2/3}\right\}^2}{\left[X_o^2 \left\{1 + (\beta t)^{2/3}\right\}^2 - 1\right]^2 + Y^2} \qquad (23)$$

where

$$X_o = \frac{\omega_{oo}}{\omega}, \quad \omega_{oo} = \frac{\pi}{L_o} \left(\frac{C}{A}\right)^{1/2}$$

L_{oo} is the initial loop length immediately after deformation, The significant feature of this expression, which does not appear in the low frequency approximation (20) and (21), is that the rate of recovery depends on the value X_o (or L_o) at which the recovery begins. In other words the rate of recovery depends on how much deformation (in terms X_o) has been induced prior to the recovery. The characteristics of these expressions (22) and (23) are plotted in Figure 21 (for attenuation) and Figure 22 (for velocity change), for the case of $f = 10^7$ cycles/sec and $B = 5 \times 10^{-4}$ c.g.s. unit. As can be seen smaller values of X_o give a slower rate of recovery of attenuation. The curve denoted by $X_o \gg 50$ corresponds to the expression for low frequency approximation (20). A velocity minimum should be observed as the recovery proceeds, when X_o is sufficiently small as shown in Figure 22.

Following the above scheme we have performed one preliminary experiment at room temperature. Figure 23 shows the stress strain, attenuation strain and fractional

---

(12) ASD-TDR-62-186, Part II

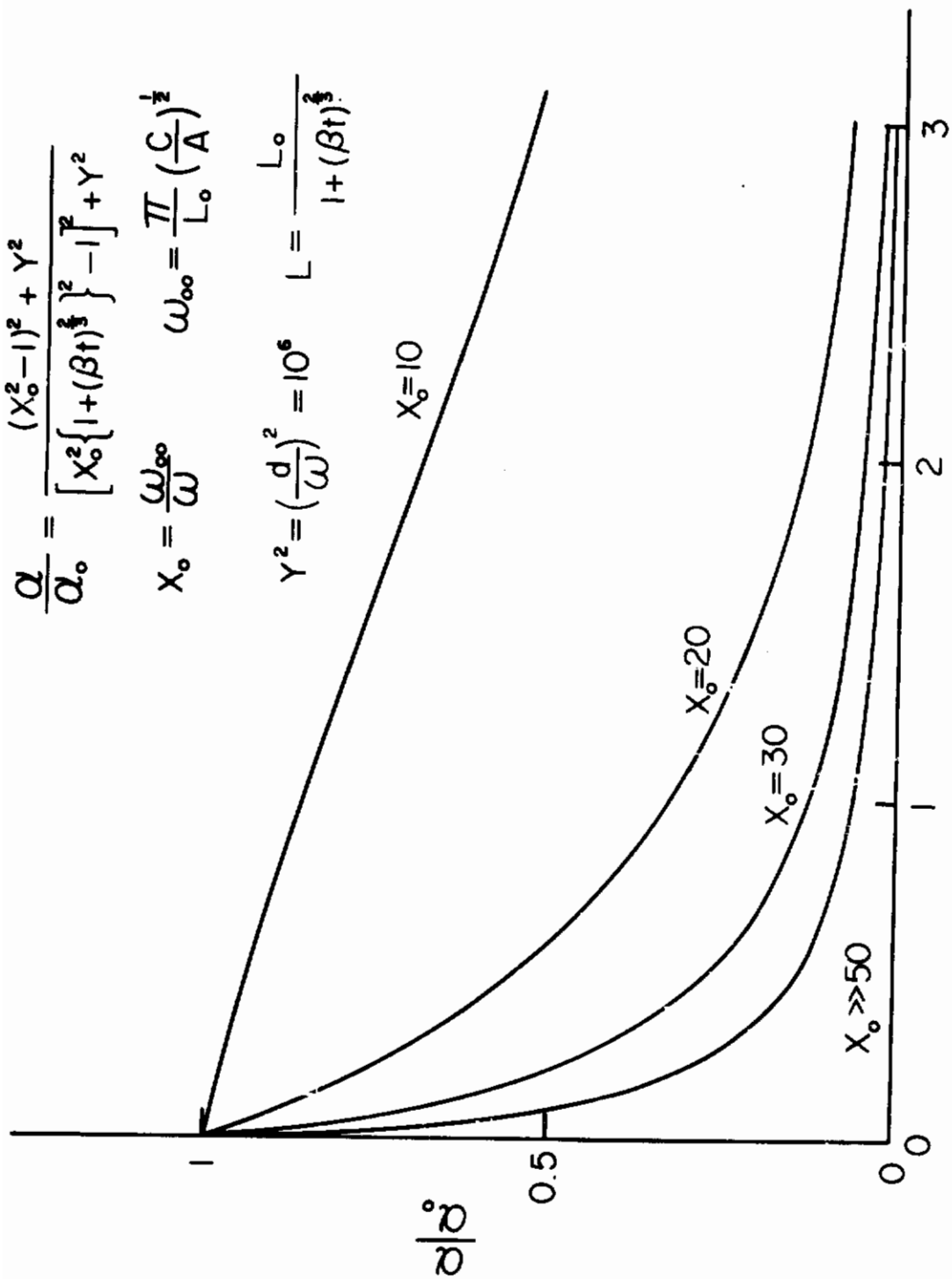

Figure 21. Recovery of Attemation After Deformation (Theoretical).

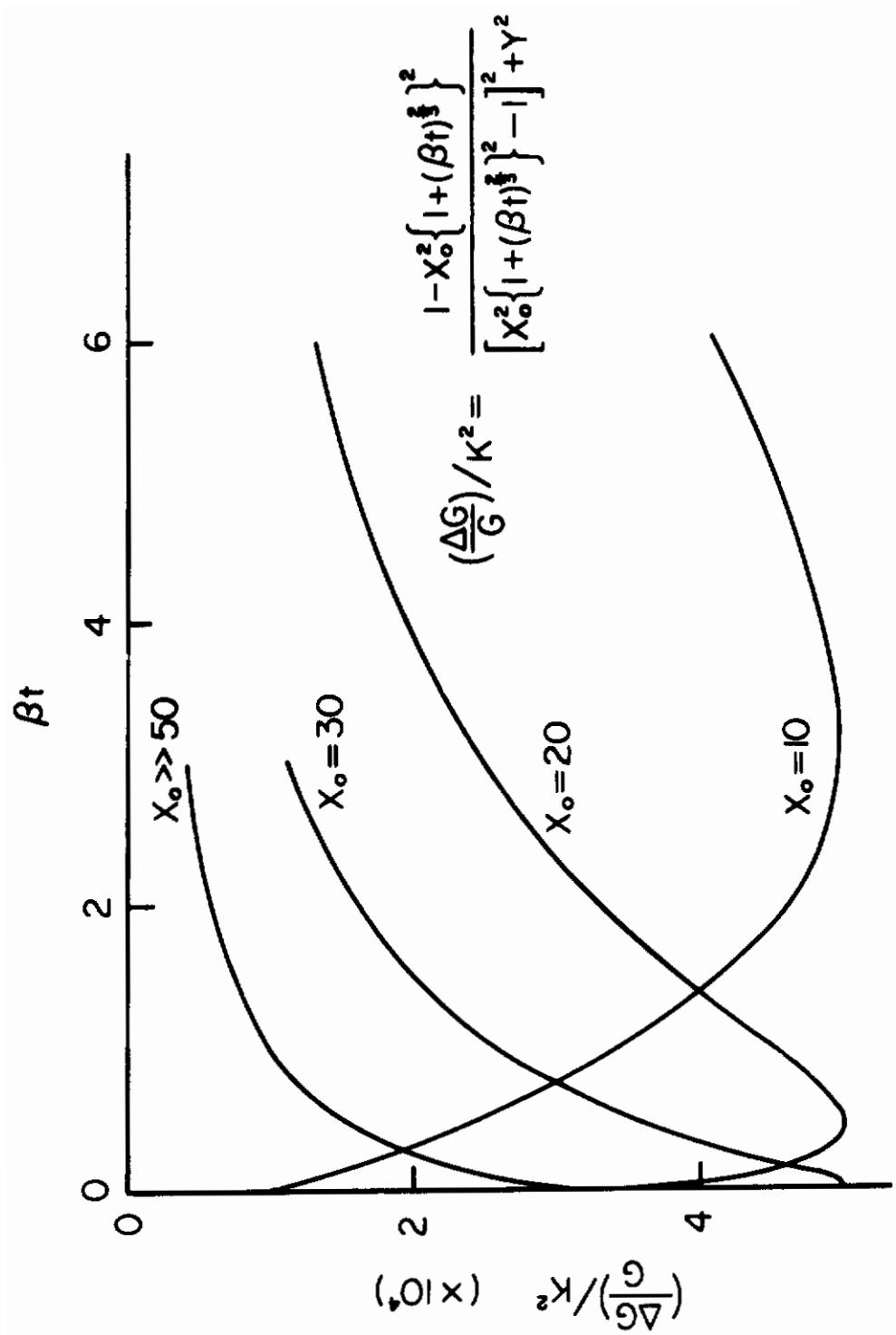

Figure 22. Velocity Change After Deformation (Theoretical).

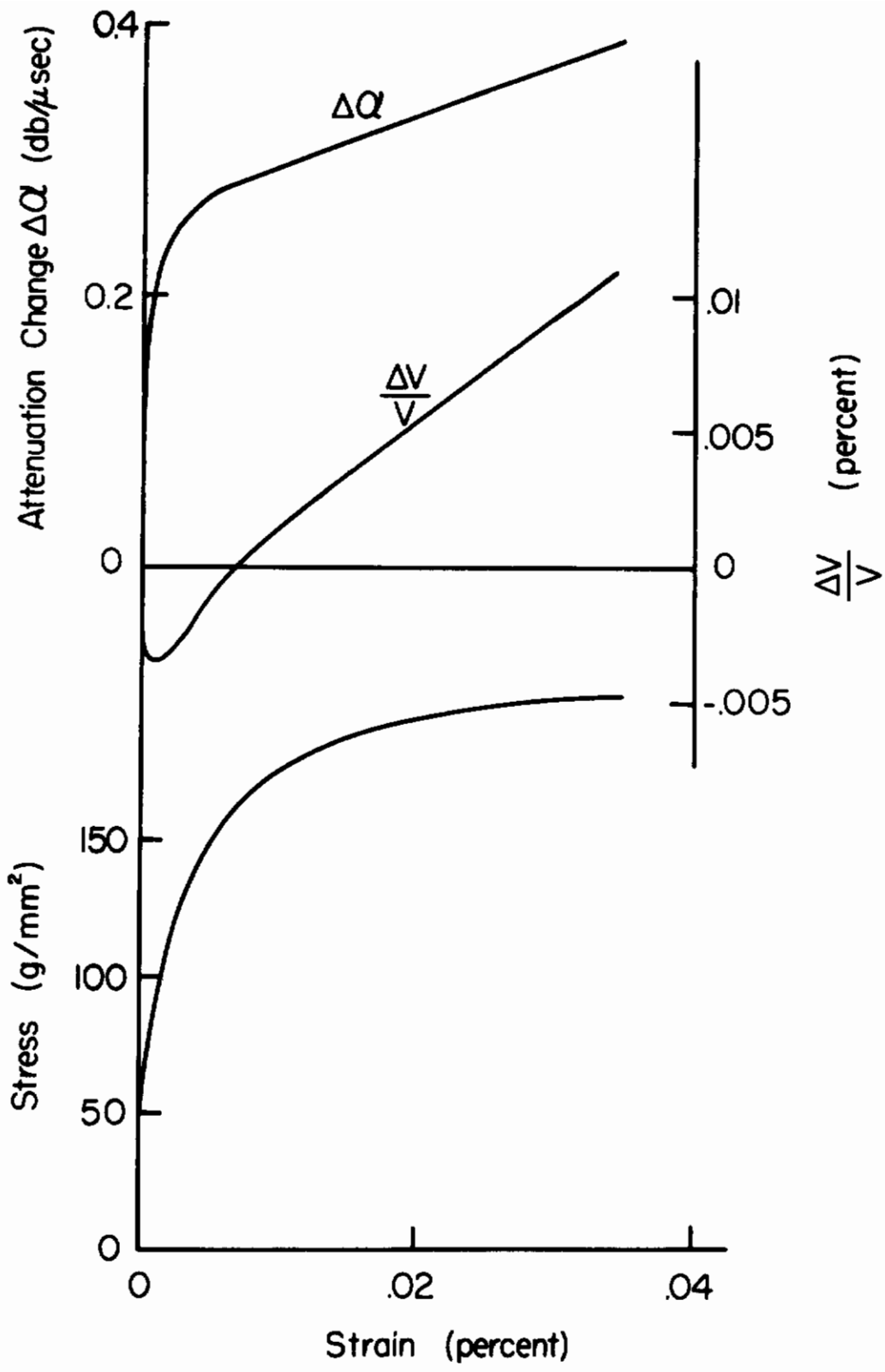

Figure 23. Attenuation Change, Velocity Change and Stress as a Function of Strain. Aluminum Single Crystal <0.5> Orientation.

velocity change-strain relationship. The results clearly show that the deformation was stopped well within a region of the velocity anomaly. This is evident because as α increases with strain (in Figure 23), values of $\Delta V/V$ are positive and examination of the formula shows this to be the anomalous range. The normal velocity effect follows as $\Delta V/V$ becomes negative, on plot shown in Figure 23.

Figure 24 shows the attenuation change as a function of time after deformation for two experiments; in one case with 0.035% deformation and in a second case with 0.67%. The orientation was the same in each case. The rate of recovery for 0.67% strain is much larger than that for 0.035% strain, which agrees qualitatively with the analysis described above.

We have also measured the recovery of velocity change. Unfortunately, however, the overall sensitivity (which includes the echo time measurements of the pulse and the elongation measurements of the specimen) is not sufficient to see whether there is a velocity minimum during recovery. We also need more accuracy and stability in recording the attenuation recovery in order to analyze the recorded curves in terms of expression (23). Attempts are being made to overcome these difficulties as well as to establish a satisfactory technique for this experiment.

Theoretical features of a recovery mechanism which takes into account the escape of pinning agents to dislocation jogs have been considered in some detail, and are discussed in what follows. Excess vacancies produced during plastic deformation interact with dislocations where the interaction energy has the form $E_j = E_{oj} \left(\frac{b}{r}\right)^j$; r is the distance between the dislocation and the vacancy, b is the Burgers vector, E_{oj} is the binding energy, j = 1,2. The value j = 1 corresponds to the interaction due to the difference in the elastic constants between vacancy region and the solid matrix. As a consequence of these interactions vacancies migrate during the recovery period to the dislocations and immobilize them against the applied oscillatory stress. During the plastic deformation, however, the moving dislocations on the glide plane will intersect other dislocations and produce jogs. These jogs act as sinks for vacancies because the vacancies can disappear to the jog by shifting the jog by one atomic distance along the dislocation line. Therefore, vacancies arriving at the dislocation through the interaction E_j will diffuse to the nearest jog and be eliminated, thus losing their identity as a pinning agent. The net concentration of vacancies responsible for the pinning, on the dislocation line will be the difference of the concentration of vacancies arriving at the dislocation and the concentration disappearing at the jogs.

Assume that $E_1 = E_{o1} \left(\frac{b}{r}\right)^1$ is the energy of interaction of a point defect with a dislocation. The defects diffuse toward the dislocation under a force $F = -(dE/dr)$, with a velocity $v = DF/kT$, where D is the diffusion coefficient of vacancies. After a time t, all the defects in supersaturation at a distance less than r, where

$$r = vt = \frac{Dft}{kT} = \frac{DE_1 tb}{kTr^2}$$

will have arrived at the dislocation. Let $C_1 + C_o$ be the initial concentration of vacancies and C_o their equilibrium concentration ($C_1 > C_o$). Their rate of arrival at the dislocation, per unit length of dislocation is

$$\left(\frac{dn}{dt}\right)_{arr.} = \frac{2\pi r\, dr}{b^3 dt} C_1 = \frac{2}{3}\frac{\pi}{b^3} C_1 \left(\frac{DE_1 b}{KT}\right)^{2/3} t^{-1/3}$$

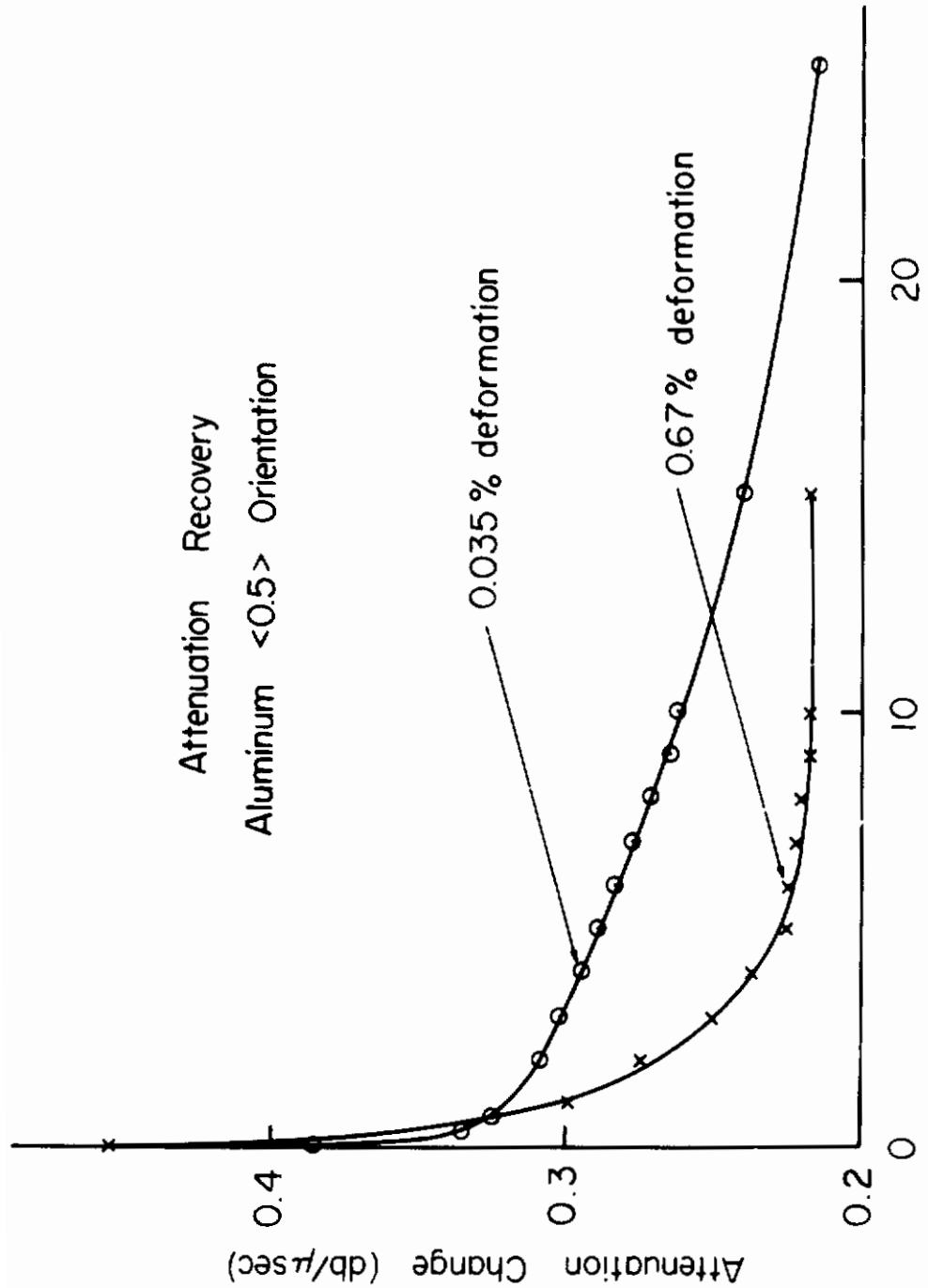

Figure 24. Effect of the Amount of Deformation on Attenuation Recovery. Aluminum Single Crystal <0.5> Orientation.

The interaction energy between a vacancy on a dislocation and a jog of the dislocation may be expressed in the following way

$$E_3 \tilde{-} E_{o3} \frac{b}{x} ,$$

where x is distance between the vacancy and the jog, $E_{o3} = E_f$ (energy of formation of a vacancy).

Using a procedure similar to that described above, the rate of escape of vacancies at the jog $(\frac{dn}{dt})_{esc.}$ per unit length of dislocation may be expressed in the following way

$$(\frac{dn}{dt})_{esc.} = \frac{2}{3} \frac{1}{\ell b} C(t) (\frac{D^1 E_f b}{KT})^{1/3} t^{-2/3}$$

where ℓ is the average distance between adjacent jogs, C(t) is the concentration of vacancies on the dislocation at time t, D^1 is the diffusion coefficient of vacancies along the dislocation line.

Therefore, the time rate $\frac{dn}{dt}$ of vacancy accumulation on a unit length of dislocation line is

$$\frac{dn}{dt} = (\frac{dn}{dt})_{arr.} - (\frac{dn}{dt})_{esc.}$$

$$= \frac{2}{3} \frac{\pi}{b^3} C_1 (\frac{DE_1 b}{KT})^{2/3} t^{-1/3} - \frac{2}{3} \frac{1}{\ell} n(\frac{D^1 E_f b}{KT})^{1/3} t^{-2/3}$$

$(\frac{c}{b} = n)$.

This differential equation has a solution of the form

$$n = \frac{A}{B}(t^{1/3} - \frac{1}{3B}) + (n_1 + \frac{A}{3B^2})e^{-3Bt^{1/3}} \qquad (24)$$

where

$$A = \frac{2}{3} \frac{\pi}{b^3} C_1 (\frac{DE_1 b}{KT})^{2/3}$$

$$B = \frac{2}{3} \frac{1}{\ell} (\frac{D^1 E_f b}{KT})^{1/3}$$

n_1 = number of vacancies on a unit length of a dislocation at time t = 0 $(n_1 = \frac{1}{b} C_1)$. When $3Bt^{1/3} << 1$ (early stages of recovery) equation (24) can be approximated in the form

$$n = (3/2)At^{2/3} \qquad (25)$$

provided that $n_1 << \frac{A}{3B^2}$. This means that in the early stages of recovery a $t^{2/3}$

law dominates. When $3Bt^{1/3} >> 1$ equation (24) can be approximated in the form

$$n = \frac{A}{B} t^{1/3} \qquad (26)$$

This means that in later stages of recovery, the recovery rate slows down (from $t^{2/3}$ to $t^{1/3}$), which is often observed in our attenuation recovery (a plot of the concentration as a function of $t^{2/3}$ deviates from a straight line toward slower rates as time t becomes larger.)

IV. Automatic Recording Time Measurement Unit

A complete assembly of the Automatic Recording Time Measurement Unit (ARTMU) is under construction. A block diagram of the unit (plus Signal Source) is shown in Figure 25 .

The instrument has been designed primarily to measure, automatically, small changes in time interval between any two ultrasonic echoes produced by means of an Ultrasonic Attenuation Comparator (13) (MKXVIII Signal Source) and suitable sample. To accomplish this measurement the entire train of echoes is amplified (after conversion to the 60 Mc/sec intermediate frequency) by two identical IF amplifiers. These IF amplifiers have gain capability of 100 db, bandwidth of 5 Mc/sec, and bandwidth and center frequency unaffected by at least 40 db gain control range. The detected (video) output of each IF amplifier is coupled to an Echo Selector (gate) where a particular echo may be allowed to pass on to the Echo Shaper; all other echoes are rejected. Time of opening of the Echo Selectors is controlled by Time Delays #1 and #2. These delays are continuously variable from 0-150 microseconds. Delay #1 is triggered by the "sync out" pulse from the MK XVIII Signal Source, and Delay #2 is triggered by the delayed output of Delay #1.

After selection each echo is amplified and used to trigger an avalanche transistor which provides a shaped output pulse having an amplitude of approximately 20 volts and a rise time of approximately 1 nanosecond. Shaped echo #1 is used to trigger simultaneously a precision Burst Generator (200 microsecond duration burst of one microsecond markers) and Time Delay #3 which is digitally varied in 1 microsecond steps from 0.7 to 200.7 microseconds. The one microsecond markers are applied to a Marker Selector (gate). The appropriate marker (between 1 and 2 microseconds before echo #2) is allowed to pass through the gate by properly setting Delay #3. (Relative time position of the various delays is known since they are fed back to the Z-axis of the MK XVIII to strobe the echo display). The selected precision marker triggers the 0-2 microseconds Saw Generator and Peak Detector; the Saw Generator is turned off sometime between 1 and 2 microseconds after it is initiated by selected echo #2. Therefore, the peak amplitude of the "saw" voltage is a linear function of the time of occurrence of the second echo (with respect to the selected marker which is digitally related to the first echo). To measure the "saw" voltage it is peak detected and applied to a high impedance differential voltmeter calibrated in appropriate units of time. Also fed into the differential voltmeter is an offset voltage which effectively makes the voltmeter insensitive to the first microsecond of operation of the saw tooth generator. This offset voltage will, therefore, allow the analog measurement to go to an artificial zero which would be impossible to obtain on a linear basis if the saw tooth had to be measured back to a true zero voltage. The total time interval measurement is obtained by adding the digital delay of Delay # 3 (14) to the time calibrated analog output of the Saw Generator and Peak Detector. The latter measurement is converted to low impedance in the differential voltmeter and is therefore capable of driving X-T and X-y recorders.

---

(13) Chick, Anderson and Truell; JASA, 32, 186, (1960)

(14) The dial of Delay #3 is adjusted to correct for the 1 microsecond error introduced by working from the 1 microsecond point on the "saw".

The sequence of operations may be followed in Figure (26). (a) and (b) are the detected output of IF #1 and IF #2 respectively where the gain of IF #1 is controlled by selected Echo #1 and the gain of IF #2 is controlled by selected Echo #2 by means of automatic gain control (AGC) circuity (15). (c) and (d) show the outputs of Delay #1 and Delay #2. Each delay is continuously variable from 1-5 microseconds. (e) and (f) show the two Selected Echoes and (g) and (h) the two selected echoes after shaping. (i) shows the Burst Generator output as initiated by shaped Echo #1. (j) shows the 200 microsecond square wave initiated by Echo #1 which determines the duration of the Burst Generator. (k) shows the output of Delay #3 which is variable in 1 microsecond steps from 0.7 to 200.7 microseconds with a 0.6 microsecond gate width output to select the appropriate precision marker as shown in (1). The Sawtooth action is initiated by the selected marker and terminated by Echo #2 as shown in (m); since the "saw" timing capacitor is also the Peak Detector Capacitor, it is necessary to discharge the capacitor to zero volts before each run up of the "saw". This is accomplished at the time of the occurrence of the leading edge of the output from Delay #3. Output from the Differential Voltmeter is a pure D. C. voltage (i.e. it does not show the "saw" run up) since the time constants involved are orders of magnitude greater than the "saw" duration.

Most sections of the unit have been extensively checked out on breadboards. The one section that has not been completely solidified to date is the Saw Generator and Peak Detector. This section has been checked on a preliminary basis using avalanche transistors as switching elements with the "saw" timing capacitor and peak detector capacitor being the same device with storage maintained by a diode. This technique works well but requires an extremely high input impedance device for the following voltmeter stage. An appropriate device has only recenly become available in the form of insulated gate field effect transistors with input impedance greater than 10^{10} ohms.

Normal resolution of the analog readout section in the 1 microsecond position will be 10 nanoseconds. However, by means of the offset voltage which is continuously variable with a ten turn potentiometer, it is possible to position the readout voltage near zero and then increase the voltmeter sensitivity by a factor of ten. Resolution would then be 1 nanosecond out of a possible time difference between echoes of 200 microseconds or 1 part in 2×10^5. Because the unit operates from the detected echoes, it may be used at any frequency where two or more high stability echoes are available

(15) AGC in some form is necessary since the time function of the echo shaping circuity is amplitude sensitive. Considerable effort was put into the IF strips to eliminate changes in center frequency and bandpass with gain. If such changes were permitted, they would produce an error in the final time measurement.

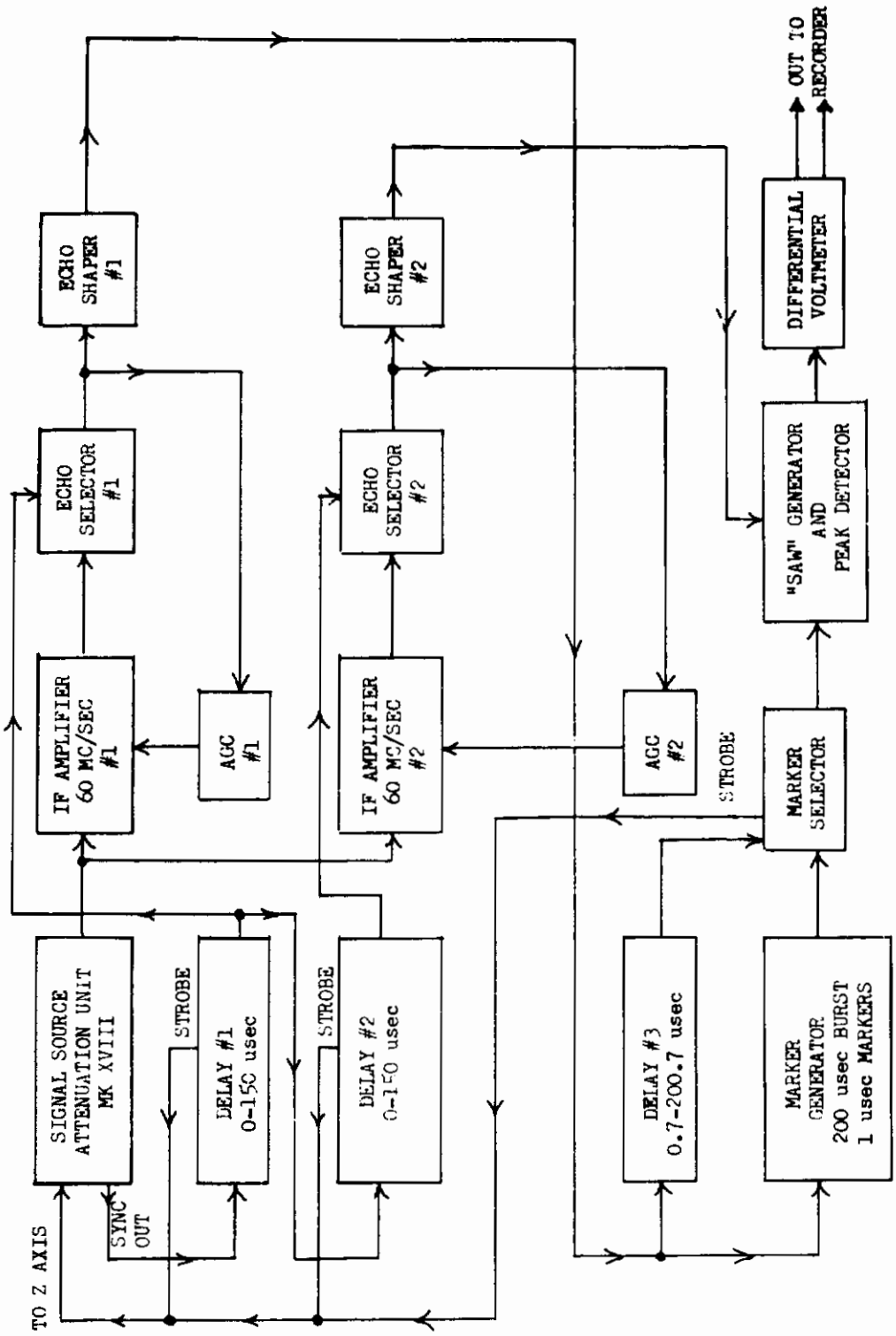

Figure 25. General Block Diagram; "Automatic Recording Time Measurement Unit" (ARTMU)

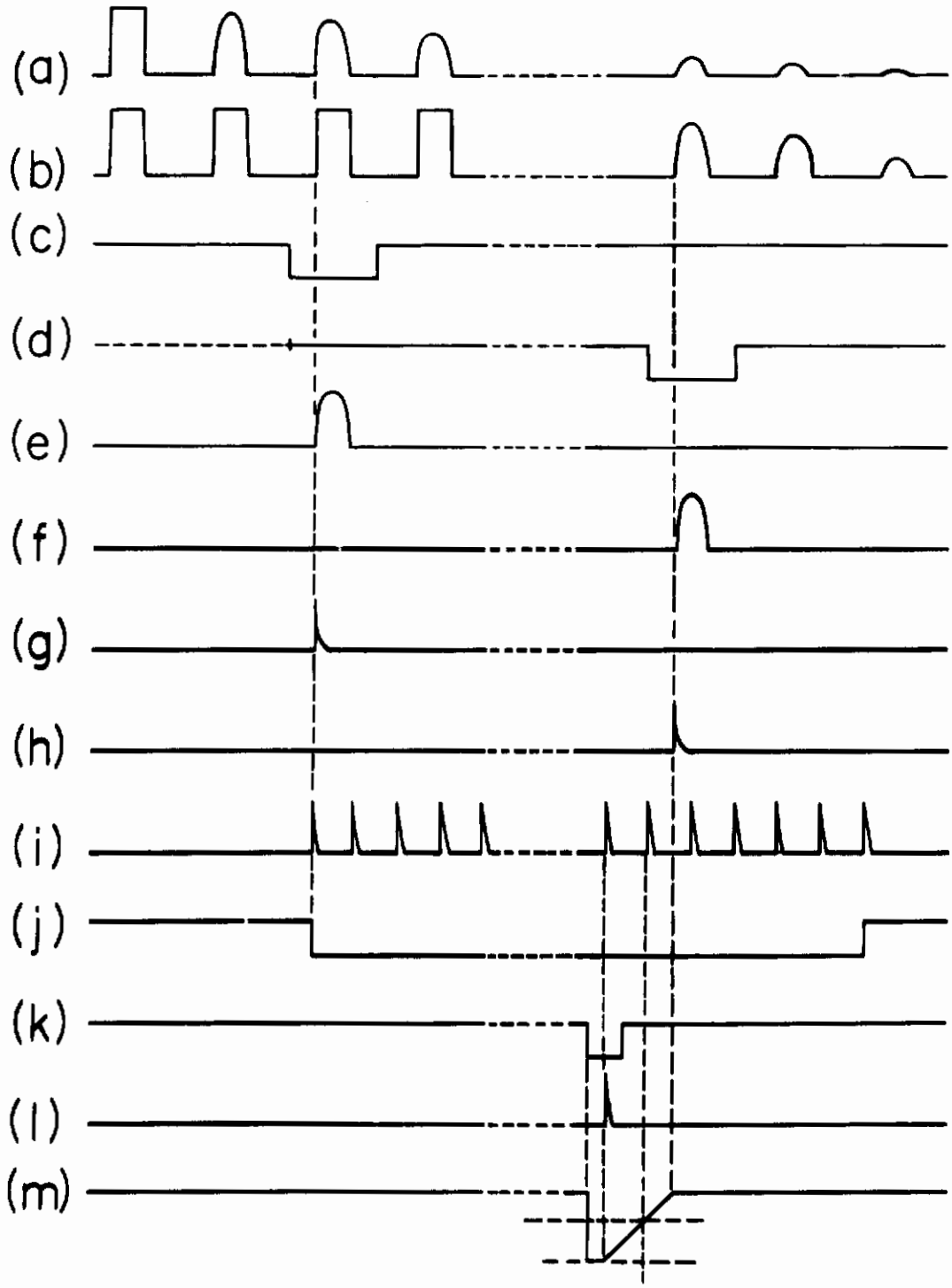

Figure 26. Time Sequence of Wave Forms in ARTMU.

V. Publications Arising Entirely or in Part from the Work of This Contract

"Dislocation Damping in Sodium Chloride"; B. B. Chick, A. Hikata, C. Elbaum and R. Truell, Applied Physics Letters 2, 5, (1963)

"Electrical Charge Study in Sodium Chloride During Plastic Deformation"; A. Hikata, C. Elbaum, B. B. Chick and R. Truell, Journal of Applied Physics 34, 2154 (1963)

"Effect of Dislocations on Finite Amplitude Ultrasonic Waves in Aluminum"; A. Hikata, B. B. Chick, C. Elbaum, Applied Physics Letters 3, 195 (1963)

"Anomalous Ultrasonic Velocity Changes in Deformation and Irradiation Induced Dislocation Pinning"; R. Truell and A. Granato, Journal of the Physical Society of Japan 18, 95 (1963), Supplement I